

**COHERENT STATES OF DAMPED OSCILLATORS AND THEIR  
RELEVANCE TO LIGHT INDUCED ULTRA WEAK PHOTON  
EMISSION IN PLANT TISSUES**

**SIVADASAN. V. A.**  
INSTITUTE OF SELF-ORGANISING SYSTEMS AND BIOPHYSICS  
**NORTH-EASTERN HILL UNIVERSITY**

THESIS SUBMITTED  
IN PARTIAL FULFILMENT OF THE REQUIREMENT  
OF THE  
**DEGREE OF DOCTOR OF PHILOSOPHY**  
IN  
**BIOPHYSICS**

OF  
**THE NORTH-EASTERN HILL UNIVERSITY**  
SHILLONG 793022, INDIA

**APRIL 2002**

**Institute of Self Organising Systems and Biophysics  
NORTH-EASTERN HILL UNIVERSITY**

I, Sivadasan V.A., hereby declare that the subject matter of the ensuing thesis is the record of the work done by me and the contents of this thesis did not form basis of the award of my previous degree to me or to the best of my knowledge to anybody else. This thesis has not been submitted by me for any research degree in any other university or institute.  
This is being submitted to the North-Eastern Hill University for the degree of Doctor of Philosophy in Biophysics.

*Satish Kumar*  
for Director

*R.P. Bajpai*  
(R.P. BAJPAI)  
Supervisor

*V.A. Sivadasan*  
( V.A. SIVADASAN )  
Candidate

**Institute of Self-Organising Systems &  
Biophysics, NEHU, Shillong,**

April 1, 2002

## ACKNOWLEDGEMENT

I consider myself extremely fortunate to work under an eminent teacher like Prof. R. P. Bajpai, whose constant encouragement and personal involvement in the problems that come up during this period has made the work presentable in this form. I acknowledge with deep sense of gratitude to him.

I take this opportunity to express my gratitude towards Prof. Satish Kumar, Prof. Vinod Singh and Prof. Debjani Roy of the Institute of Self Organising Systems and Biophysics for their timely advice and help at various stages of this work.

I hereby acknowledge Prof. Y. S. Jain of the Physics department of N.E.H.U. for advising me to pursue a research carrier in photonics in the Institute of Self Organising Systems and Biophysics. I thank Prof. M. K. Parida, Prof. P.N. Pandita and Prof. Y. S. T. Rao of the Physics department N.E.H.U. for their interest in the satisfactory completion of the work.

I hereby by acknowledge Dr. Anil Kumar Mavila, Dr. Ranjit Singh Chingakhm Dr. Bijoy Lakshmi Borah and P. Asha Chingakhm for their interest and support in completing the work.

I am thankful to Prof. B.B.P. Gupta from Zoology, Dr. S. Sarma from Geography and Mr. N.P. Garg from engineering section for the constant encouragement and support. I sincerely thank Dr. S. Aravamudhan of Chemistry department N.E.H.U. for MATHCAD applications.

I hereby acknowledge with deep sense of gratitude to my sisters Seetha, Devi, and Rajumol for their moral and financial support that they have extended.

This column remains incomplete if I forget to acknowledge Mr. Unni Rajan, Mr. K. Sharma, Mr. A. Thomba Singh, Mr. O.P. Thripati, Mr. Sivaprakasan, Thomas K. Job, Mrs. Florence and Mr. Vijayan for their timely help whenever needed.

Shillong

Dated April 1, 2002

  
( V.A. SIVADASAN )

## Table of contents

<b>1. Chapter 1: Status of Biophoton research</b>	<b>1</b>
1.1 Introduction	1
1.2 Unexplained Features of Biophoton signals	1
1.3 Signals of Delayed Luminescence	5
1.4 Light induced biophoton emission	7
1.5 The complete biophoton signal	11
<b>2. Chapter 2 Classical and Quantum description of the Electromagnetic Field</b>	<b>12</b>
2.1 Introduction	12
2.2 Classical description of electromagnetic field	12
2.3. Quantum description of electromagnetic field	15
2.4 Popular states of electromagnetic field	17
2.5. Non-classical properties of light	27
2.6 Non-local properties of electromagnetic field	30
Figures	33
<b>3. Chapter 3: Properties of states obtained after squeezing and displacing number states</b>	<b>36</b>
3.1. Introduction	36
3.2. Popular States of Electromagnetic Field	36
3.3. States obtained by squeezing and displacing number states	39
3.4. Squeezed and displaced states of electromagnetic field	41

3.5. Some General Comments about the Expectation Values	44
3.5. Minimum Uncertainty Character of the States	49
3.7. Photo Count Distributions of Different States	51
Figures	54
<b>4. Chapter 4: A Phenomenological Model of Biophoton Emission</b>	<b>70</b>
4.1 Introduction	70
4.2. Biophoton Emission from a Coherent Light Field	72
4.3 Description of Biophoton Field by a Damped Harmonic Oscillator	74
4.4 Mathematical formulation of the model	78
<b>5. Chapter 5: Biophoton signal from <i>Tagetes Patula</i></b>	<b>88</b>
1.1 Implications of the model	88
5.2 Biophoton Signal of <i>Tagetes Patula</i>	90
Figure	94
<b>6. References:</b>	<b>95</b>

## Chapter 1

### Status of Biophoton research

**1.1 Introduction:** Living systems from bacteria to human tissues continuously emit photons with an ultra weak flux mainly in the visible region <sup>[1-4]</sup>. The flux of photons is 12 to 15 orders of magnitude lower than that emitted by similar non-living systems in allowed electromagnetic transitions. Both living and non-living detectors can detect the presence of such a low intensity flux. The detection by living material like yeasts, onion roots, etc. is qualitative and requires long time exposure. In contrast, the detection by non-living material is quantitative and fast. The development of photon counting techniques in single photon mode allows detection of photon flux having energy of the order of  $10^{-17}$ W by employing large single crystal scintillation detectors that are sensitive to a broad spectral band and have dead time of around  $1\mu\text{s}$ . Crystals sensitive to different spectral regions are available and it is observed that crystals sensitive to the photons in the visible region register much larger fluxes of photons from living objects. This is considered as sufficient to infer that living systems mainly emit photons in the visible range. The scintillation crystal sensitive to photons in the wavelength band (300-800) nm is considered the most appropriate detector of photons emitted by living systems.

**1.2 Unexplained Features of Biophoton signals:** The three features of photon emission from living systems mentioned above namely, emission in the visible range, almost constant and non-decaying flux, and ultra weak intensity, are widely observed. These features are incomprehensible in the standard framework of

photon emission. In the standard framework, photon emission arises from the quantum jump of an electron from a higher energy state to a lower energy state; the difference of energy between states is emitted as photon of definite wavelength. The framework requires a mechanism for pumping electrons (or charges) from a lower energy state to a higher energy state;. The emission of photon with wavelength in the visible range requires a few electron volts ( $\approx 3-5$  eV) of energy difference between electronic states. The energy supply in living system is controlled by ATP-ADP biochemical reaction; each reaction supplies around 0.01eV of energy. So that the excited state of an electronic system produced by a single biochemical reaction can emit photon only in infrared region. Photon emission in the visible or UV region will require a mechanism for up converting the energy by exciting a state from cumulative actions of many elementary biochemical reactions. The mechanism for up converting biochemical energy has to be operative all the time in every living system. Such a mechanism has not been identified so far. The constant and non-decaying photon flux is also a problematic feature for the standard framework. Each quantum jump of the standard framework depletes the number of electrons occupying the higher energy state; the depletion decreases the signal strength purely from statistical considerations. The decrease is observed as exponential decay of the signal. Each signal has to decay. Any non-decaying portion in a signal implies the existence of a mechanism to recoup the electrons of the higher energy state lost in quantum transitions. No mechanism for recouping these electrons has been identified so far. Finally ultra weak intensity implies that the transition arises either from some

unforeseen errors and is a rare event or from the cooperative functioning of many molecules and is indicative of a new mechanism operating in living systems. The unforeseen errors are likely to occur randomly while a new mechanism is likely to leave some signatures. The measurement of photo count statistics perhaps, can discriminate between them. The distribution of photo counts in majority of low intensity photon signals from living systems appears to be Poisson; there are also a small number of cases with sub and super Poisson distributions. The distribution of photo counts does not appear to be normal; which is considered as an indication that these signals are not consequences of random errors. Perhaps, some unknown mechanism is responsible for these signals. Since the unknown mechanism appears to be operative only in living systems, the mechanism might be playing some role in the emergence or sustenance of “life”. If it is so, then the photon signals can provide information about the unknown mechanism and about the emergence or sustenance of “life”. This potentiality is emphasized by adding a prefix bio to the photons of unknown origin emitted by living systems; these photons are, therefore, called biophotons. Biophotons are expected to have biological relevance and origin; which need to be uncovered. The uncovering encounters many problems, which arise from the ongoing changes in a living system, the low strength of the biophoton signal, and the absence of structure in the biophoton signal.

A living system is a dynamical object, which changes continuously and undergoes an irreversible evolution. These changes preclude repetition of a measurement under identical conditions. A living system also requires an

interacting environment with ambient temperature in the range ( $5^{\circ}\text{C}$  -  $40^{\circ}\text{C}$ ) for its survival and functioning. The environment and its interaction with the system can also emit photons. It is difficult to isolate a living system from its environment for observing biophoton emission. A system, its environment and the photon detector generate noise in the temperature range mentioned above. The detector can be isolated and kept at lower temperature; still its contribution to noise is substantial. The state of the art detectors used in biophoton measurements show noise of around 10-counts/s. The noise is comparable to the observed strength of less than 10 counts/s in biophoton signals. Since noise is comparable to the strength of a biophoton signal of unknown origin, the inferences drawn from such measurements about the properties of biophoton signals are usually considered indicative and not conclusive. Another reason for this state of affair is the absence of any structure in a biophoton signal. The signal is flat and its intensity does not vary with time. The signal, therefore, has only one measurable quantity - its strength- to carry information. The deciphering of this information requires an absolute determination of intensity, which is quite difficult because of substantial background noise. Consequently, low intensity biophoton signals of nearly constant strength have not been properly investigated and their implications have remained unexplored. Attempts were even made to deny their existence and to attribute observations to some experimental artefacts in the earlier phase of investigations. So much so, that Alexander Gurvich who was the first to observe biophotons in his laboratory and to realize their biological relevance was considered a false prophet <sup>[5]</sup>.

**1.3 Signals of Delayed Luminescence:** The importance of the phenomenon of biophoton emission increased considerably after the inclusion of another class of photons emitted by living systems in its fold. The photons in the new class are emitted after an exposure of a living system to light and are mainly in the visible range. These photons do not emanate from the phenomena of fluorescence and phosphorescence well known in non-living systems. Almost all non-living systems exhibit the phenomenon of fluorescence. The signal of fluorescence is very intense for a short while but its intensity decreases rapidly. The signal is observable only for a few microseconds after exposure of a system to light; it becomes negligible and undetectable in a few milliseconds. The phenomenon is observable in living systems as well. The UV and visible fluorescence spectroscopy utilises this phenomenon to identify a living system and its various non-living constituents. The phenomenon of phosphorescence is so not ubiquitous; it is observable only in a few non-living substances. The signal of phosphorescence is observed after a delay that can range from a few milliseconds to days. The nature of decay of its signal is exponential and the characteristic features of its signal are delay time, wavelength and decay parameters. These features can easily identify a signal emanating from the phosphorescence phenomenon. Such signals have been observed in a few living systems and these signals are attributable to the phosphorescence of non-living constituents. Strehler and Arnold <sup>[6]</sup> were the first to observe that photosynthetic tissues after exposure to light continue to emit a decaying photon signal of weak intensity for a few minutes. The characteristics of this weak photon signal were such that they could

not attribute it to either fluorescence or phosphorescence. They suggested that the weak photon signal emanate from a new phenomenon and called it-delayed luminescence. It was subsequently found that the phenomenon of delayed luminescence is not restricted to photosynthetic tissues alone but is observable in almost all living systems from bacteria to human tissues. The signal of delayed luminescence is easily observable in photosynthetic tissues because it is more intense and of larger duration. The signal is observable for time intervals of the order of 100s. The signal in other plant tissues is less intense but is observable for similar time intervals with detectors that are more sensitive. The signal in other living systems is much weaker and is observable only for duration in the range of 1ms to 10s. The delayed luminescence signal cannot be observed in the time interval less than 1ms because of the presence of strong fluorescence signal. The distinguishing feature of all delayed luminescence signals is their decay behaviour. The nature of decay is not exponential; it is probably hyperbolic. As pointed out earlier, the non-exponential nature of decay is an intriguing feature in any system for it requires a new framework for description. Such a decay can originate from cooperative behaviour of emitting units. Another aspect of the signal of delayed luminescence is its sensitivity to many physiological and environmental factors. The sensitivity highlights the biological relevance of the signal. Non-exponential nature of decay and sensitivity to physiological parameters are good enough reasons for the assertion that the signal of delayed luminescence is also a type of biophoton signal. There are, therefore, two types of biophoton signals- one type is emitted spontaneously and other type after

exposure to light. These signals are named spontaneous and stimulated biophoton signals and they emanate respectively from spontaneous and stimulated biophoton emissions.

**1.4 Light induced biophoton emission:** The investigations of stimulated biophoton emission is more fruitful because of the following reasons:

1. The stimulated biophoton signal is usually 2 to 3 orders of magnitude more intense than the spontaneous biophoton signal in a living system. A signal of higher intensity is easy to detect; the contribution from the background noise in its measurements is very small and almost negligible.
2. The shape of a stimulated biophoton signal provides a new feature for investigations. The signals emitted by different living systems have shapes with similar broad features but different finer details. The broad features are used in identifying a biophoton signal, while finer details in gaining information specific to the state of a system.
3. The decay shapes of stimulated biophoton signals are determined by non-invasive measurements that are completed in a small interval. These measurements can be made repeatedly.

Consequently, the phenomenon of stimulated biophoton emission has been extensively investigated. The shape of the signal and its variation with various parameters has been experimentally observed. These observations have remained qualitative for it is not been possible to quantify a biophoton signal and extract its

relevant parameters from the data. The signal is specified by means of phenomenological parameters like shape, strength, and duration. We do not have the proper framework to specify the shape of a non-exponentially decaying signal. In the absence of the framework, the different descriptions of the shape are merely arbitrary parameterisations and lack physical significance. Superimposing one signal on another after varying scales compares the shapes of two signals. The number of counts in an interval around a predefined time after exposure is used as a measure of strength. There can be many such measures. Different groups use different measures depending upon the settings of their equipments. In contrast, the duration of decay of a biophoton signal is easy to specify; we specify it by the time in which intensity of the signal decays to 10% of its starting measurable value. The observed duration of the stimulated signals varies from system to systems; it lies in the range (1ms –200s). The duration is much larger in plant tissues, where it is the range (100-200) s. The older detectors that used a mechanical shutter to regulate the collection of photons accurately determined the decay signals of duration larger than 10s. A mechanical shutter takes time of the order of 10ms in opening and closing, which makes measurements of photon counting erroneous for time intervals less than 100ms. A larger time interval offsets the effect of time spent in opening or closing the shutter. It is found that the measurements become reasonably accurate in intervals greater than 100ms. These detectors, therefore, map the decay region of a signal using points of 100ms width. The mapping averages out the finer structures of up to 100ms duration. The averaging out procedure inherent in the measurements makes the technique

suitable for determining the shapes of the signals of duration larger than 10s only. The shape of a signal of smaller duration is not well determined; only its intensity is measurable. Consequently, these detectors were unable to establish the non-exponential nature of decay of stimulated biophoton signals in many living systems. The situation changed with the use of electronic acquisition of data. The electronic acquisition allows counting the number of photons in much smaller intervals; the lower limit of measuring interval is set by the dead time of the detector. The dead time of scintillation detectors is of the order of  $1\mu\text{s}$ , so that scintillation detectors using a mechanical shutter and an electronic acquisition system are now able to establish the non-exponential nature of stimulated biophoton signals of duration greater than 1ms. The electronic acquisition of the data offers the possibility of measuring photo count statistics in a small region of slowly decaying biophoton signals of plant tissues. The duration of decay in these signals is more than 10s and one can assume the signal non-decaying in intervals of 100ms. In each of these intervals, it is possible to determine photo count statistics using measuring intervals of 10 to  $100\mu\text{s}$ . The stability and robustness of the samples is another reason for using plant tissues in investigations of biophoton signals. These samples do not require costly and elaborate controls.

Living systems, therefore, appear to emit two types of biophoton signals - spontaneous and stimulated biophoton signals. A spontaneous biophoton signal is ultra weak, unchanging and lasts for the entire life time of a living system, while a stimulated biophoton signal is weak, shows a characteristic decay structure and lasts only a small duration of less than a few minutes. The complete signal of

spontaneous emission can be measured only once in a living system, though its intensity can be measured repeatedly. A stimulated biophoton signal is assumed to be of short duration and can be observed repeatedly. Since the intensity of its signal changes with time and it is not possible to make repeated measurements of intensity in a stimulated biophoton signal. Repeated measurements of intensity are required for a determination of the statistical properties of the emitted radiation like photo count statistics and correlation coefficients. As a result, statistical properties are determinable only in spontaneous biophoton signals. The usual set up using one detector can measure two quantities in a spontaneous biophoton signal – intensity of the signal and its photo count statistics. A reasonable determination of photo count statistics requires that the physiological state of the system remains unaltered in nearly 1000 measurements of intensity. It is long time and many living systems change in this duration. As a result, the photo count statistics has been determined only in a few stable systems. The three popular distributions for the description of photo count statistics are Poisson, normal and geometrical. The specification of Poisson distribution requires one parameter namely the average intensity. The specification of normal and geometrical distributions requires two parameters namely average intensity and its variance. Average intensity and its variance are equal in Poisson distribution; the near equality holds irrespective of the number of points in a sample. In contrast, variance decreases with the number of points in the sample in normal distribution and is much less than average value. This is also true for geometrical distribution. Average intensity is nearly equal to the variance of intensity in most of the

observed spontaneous biophoton signals. It is, therefore, general practice to ascertain whether an observed distribution is sub or super or simply Poissonian. It is ascertained by calculating the Q value of the set of observations. Q values are easy to calculate theoretically for different quantum states.

**1.5 The complete biophoton signal:** The separation of the two types of biophoton signals is not easy. One cannot rule out a single biophoton signal manifesting as two different signals. Decaying part is identified as stimulated biophoton emission and long almost non-decaying tail as spontaneous signal. We give below an artist representation of the signal in Fig. 1 that summarises various regions of a typical biophoton signal. It may be noted that the figure is not to scale.

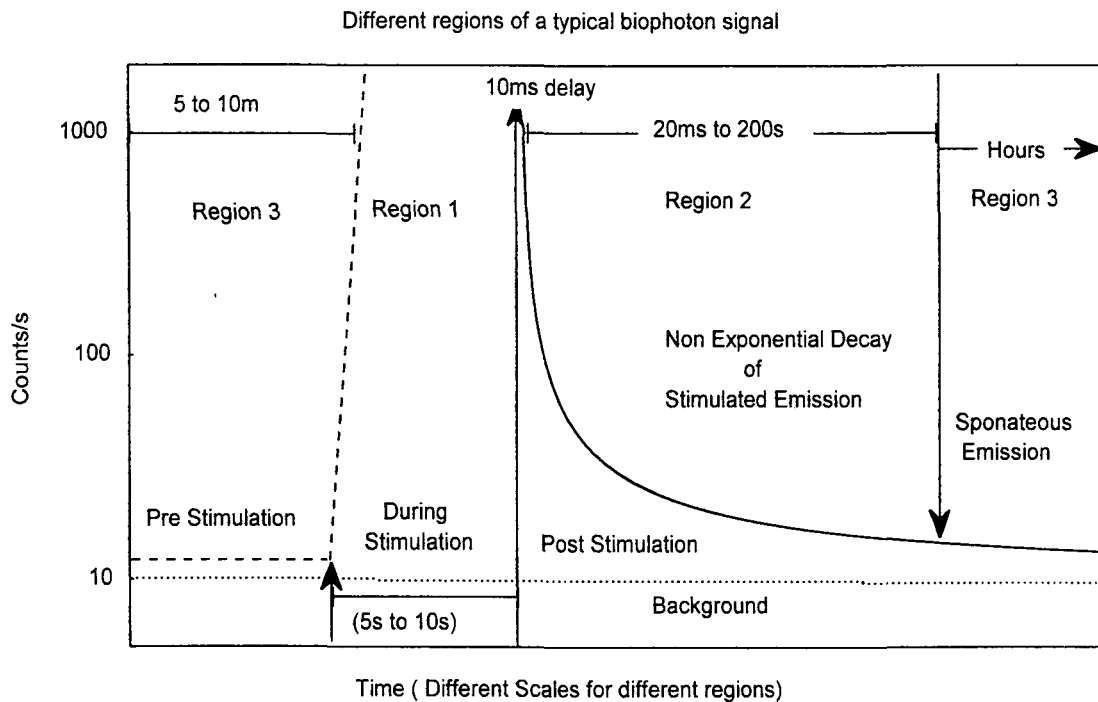


Fig.1 The different regions of a biophoton signal are shown separately. It is not possible to observe the portion of the signal during light stimulation.

## Chapter 2

### Classical and Quantum description of the Electromagnetic Field

**2.1 Introduction:** Visible light is a kind of radiant energy that produces the sensation of vision. The nature of radiant energy is electromagnetic and it forms a part of the spectrum that extends from  $\gamma$ -rays to radio waves. Classically, electromagnetic radiation is produced by the acceleration of electric charges and prevails as a means for transmission of energy and information from one place to another through empty space.

**2.2 Classical description of electromagnetic field:** Classical electromagnetic theory, put forward by Maxwell in 1860's, could explain all the known optical phenomena at that time. Electromagnetic field in the absence of charged particles and conduction currents is called free field and is described by the four Maxwell's equation <sup>[7]</sup>.

$$\nabla \times \mathbf{H} = \frac{\partial \mathbf{D}}{\partial t} \quad (1)$$

$$\nabla \times \mathbf{E} = - \frac{\partial \mathbf{B}}{\partial t} \quad (2)$$

$$\nabla \cdot \mathbf{B} = 0 \quad (3)$$

$$\nabla \cdot \mathbf{D} = 0 \quad (4)$$

Where  $\mathbf{E}$ ,  $\mathbf{B}$ ,  $\mathbf{D}$  and  $\mathbf{H}$  are the electric field strength, magnetic induction, electrical displacement and the magnetic field strength respectively. The four vectors are not independent but are related by the constitutive relations.

$$\mathbf{B} = \mu_0 \mathbf{H} \quad (5)$$

$$\mathbf{D} = \epsilon_0 \mathbf{E} \quad (6)$$

, where  $\epsilon_0$  is the electrical permittivity and  $\mu_0$  the magnetic permeability of vacuum.

These relations permit to take E and H to be independent vectors. They satisfy the wave equation i.e.

$$\nabla^2 \mathbf{E} = \frac{1}{c^2} \frac{\partial^2 \mathbf{E}}{\partial t^2} \quad (7)$$

$$\nabla^2 \mathbf{H} = \frac{1}{c^2} \frac{\partial^2 \mathbf{H}}{\partial t^2} \quad (8)$$

Where

$$c = \frac{1}{\sqrt{\mu_0 \epsilon_0}} \quad (9)$$

The solutions of (1-4) represent electromagnetic waves <sup>[8]</sup> travelling with speed c in free space. The properties described by Maxwell's equations constitute the classical properties of light. The well-known properties are:

1. The disturbance that propagates is the vibrations of electric and magnetic fields, which are orthogonal to each other.
2. The electromagnetic waves of wavelengths lying in the range (3800-6800)<sup>0</sup>A constitute Light. Light wave of a definite colour has definite frequency or wavelength.
3. Light waves travel with a constant speed in a medium, irrespective of frequency and wavelength.
4. Amplitude of the light wave is related to intensity and also to the energy crossing at a point.
5. Light can be polarized; the vibration of the electric field gives the state of the polarization.

6. When two light waves act simultaneously at a point, then the electric field at the point is given by the algebraic sum of the electric fields of two light waves. At all other points the two light waves continue to propagate without being affected by presence of each other.

The description of the electromagnetic field by  $\mathbf{E}$  and  $\mathbf{H}$  is not suitable for quantization. However, an alternative formulation in terms of electromagnetic potential,  $\mathbf{A}$  is more appropriate for quantization. Maxwell's equations are gauge invariant and in case of source free field one may choose Coulomb gauge in which both  $\mathbf{B}$  and  $\mathbf{E}$  are given by the vector potential. The fields in the Coulomb gauge are given by

$$\mathbf{B} = \nabla \times \mathbf{A} \quad (10)$$

$$\mathbf{E} = -\frac{\partial \mathbf{A}}{\partial t} \quad (11)$$

By substituting (9) and (10) in (2) and by using the coulomb gauge condition  $\nabla \cdot \mathbf{A} = 0$  it can be shown that vector potential also satisfy the same wave equation

$$\nabla^2 \mathbf{A}(\mathbf{r}, t) = \frac{1}{c^2} \frac{\partial^2 \mathbf{A}(\mathbf{r}, t)}{\partial t^2} \quad (12)$$

The solution of the above equation can be separated into positive and negative frequency parts. The vector potential  $\mathbf{A}(\mathbf{r}, t)$  can, therefore, be written as a sum of two complex terms

$$\mathbf{A}(\mathbf{r}, t) = \mathbf{A}^+(\mathbf{r}, t) + \mathbf{A}^-(\mathbf{r}, t) \quad (13)$$

Where  $\mathbf{A}^+(\mathbf{r}, t)$  contains the amplitude which vary as  $e^{-i\omega t}$  for  $\omega > 0$  and  $\mathbf{A}^-(\mathbf{r}, t)$  contains all amplitudes which vary as  $e^{+i\omega t}$ . The values of  $\mathbf{A}^+(\mathbf{r}, t)$  and  $\mathbf{A}^-(\mathbf{r}, t)$  at each point are independent coordinates and constitute denumerable set of infinity. It is more convenient to deal with discrete set of variables in finite space than the whole

continuum. Restricting the field to finite volume in space achieve this. The volume can be chosen to possess appropriate symmetric boundary conditions. The boundary conditions on a cube describe the vector potential in terms of discrete set of orthogonal mode functions.

$$\mathbf{A}^+(\mathbf{r}, t) = \sum_{\mathbf{k}} c_{\mathbf{k}} \mathbf{u}_{\mathbf{k}}(\mathbf{r}) e^{-i\omega_{\mathbf{k}} t} \quad (14)$$

$$\mathbf{A}^-(\mathbf{r}, t) = \sum_{\mathbf{k}} c_{\mathbf{k}}^* \mathbf{u}_{\mathbf{k}}^*(\mathbf{r}) e^{i\omega_{\mathbf{k}} t} \quad (15)$$

Where the Fourier coefficients  $c_{\mathbf{k}}$  are constants for a free field. The set of mode functions depends on the boundary conditions of the physical volume under consideration. The vector potential now can be written in the form <sup>[8]</sup>

$$\mathbf{A}(\mathbf{r}, t) = \sum_{\mathbf{k}} \left( \frac{\hbar}{2\omega_{\mathbf{k}} \epsilon_0} \right)^{\frac{1}{2}} \left[ a_{\mathbf{k}} \mathbf{u}_{\mathbf{k}}(\mathbf{r}) e^{-i\omega_{\mathbf{k}} t} + a_{\mathbf{k}}^* \mathbf{u}_{\mathbf{k}}^*(\mathbf{r}) e^{i\omega_{\mathbf{k}} t} \right] \quad (16)$$

And the electric field can be written in the form

$$\mathbf{E}(\mathbf{r}, t) = i \sum_{\mathbf{k}} \left( \frac{\hbar \omega_{\mathbf{k}}}{2\epsilon_0} \right)^{\frac{1}{2}} \left[ a_{\mathbf{k}} \mathbf{u}_{\mathbf{k}}(\mathbf{r}) e^{-i\omega_{\mathbf{k}} t} - a_{\mathbf{k}}^* \mathbf{u}_{\mathbf{k}}^*(\mathbf{r}) e^{i\omega_{\mathbf{k}} t} \right] \quad (17)$$

Where  $a_{\mathbf{k}}$  and  $a_{\mathbf{k}}^*$  are the complex Fourier amplitudes in classical electromagnetic field theory.

### 2.3. Quantum description of electromagnetic field:

In 1900 Max Planck showed that emission and absorption of light occur in finite units of energy known as quanta. This initiated the beginning of quantum theory, which describes the particles that make up matter and how they interact with each other and with energy. Quantum theory deals with the behavior of universe on a much smaller scale of microscopic particles and is more general than classical physics. It could be

used to predict the behavior of any physical, chemical and biological system. The main features of quantum theory of light are

1. Matter and radiant energy in the universe are described in terms of a single indivisible unit called quanta or photon.
2. It explains the phenomenon of interaction between radiation and matter that changes the form of energy.
3. It describes the wave and particle behavior at the subatomic level using the concept of wave particle duality.
4. Quantum theory describes elementary particles that have their corresponding wavelengths and quantum fields.
5. It views light as a stream of photons capable of interacting with quantum fields of charged particles and also mediates the interaction between charged particles. Interaction of radiation with matter and photon mediated electron-electron interaction may be cited as examples

Photon is the particle like excitation of electromagnetic field. It is an elementary particle having zero rest mass that carries energy, linear and angular momenta. Photon is the carrier of electromagnetic force between charged particles. They communicate with matter via interactions with electrons in atoms. Energy and momentum are the properties that allow photons to affect other particles when they collide with them. The product of Planck's constant and the frequency of a photon gives its energy. Energy of a photon corresponding to the visible light is of the order of a few electron volts. Photons exert extremely small amount of pressure when they strike a surface due to their momentum.

Quantisation of electromagnetic field <sup>[8]</sup> is achieved by treating the complex Fourier amplitudes  $a_{\mathbf{k}}$  and  $a_{\mathbf{k}}^+$  as quantum operators satisfying the usual commutation relations for bosons. An ensemble of independent harmonic oscillators may represent a typical source of electromagnetic field. A simple harmonic oscillator with unit mass and frequency,  $\omega$  can represent the behavior of an electromagnetic field. Such a harmonic oscillator is assigned to individual modes of a cavity field <sup>[6]</sup> restricted to a definite volume of space where there is no refracting material. The operators  $a_{\mathbf{k}}$  and  $a_{\mathbf{k}}^+$  have the role of exciting or de-exciting a mode of index,  $\mathbf{k}$  by one quantum of energy and are respectively known as photon annihilation and creation operators.

#### 2.4 Popular states of electromagnetic field:

**The number states:** The above defined creation and annihilation operators for a photon in a single mode can be expressed in terms of position and momentum operators  $\mathbf{P}$  and  $\mathbf{Q}$  as follows

$$a = \frac{1}{\sqrt{2\hbar\omega}}(\mathbf{Q} + i\mathbf{P}) \quad (18)$$

$$a^+ = \frac{1}{\sqrt{2\hbar\omega}}(\mathbf{Q} - i\mathbf{P}) \quad (19)$$

, where the mode index  $\mathbf{k}$  is dropped for ease of notation. These operators are non-Hermitian and satisfy the boson commutation relations i.e.

$$[a, a^+] = 1; \quad [a, a] = 0; \quad [a^+, a^+] = 0. \quad (20)$$

By inverting (18) and (19) we may write them in terms of  $a$  and  $a^+$

$$\mathbf{Q} = \sqrt{\frac{\hbar}{2\omega}}(a + a^+) \quad (21)$$

$$\mathbf{P} = i\sqrt{\frac{\hbar\omega}{2}}(a^+ - a) \quad (22)$$

Such that

$$[\mathbf{Q}, \mathbf{P}] = i\hbar \quad (23)$$

They represent the real amplitudes, p and q of two quadrature components of electric field. Electric field in terms of p and q may be written as

$$\mathbf{E}(t) = E_0[\mathbf{Q} \cos \omega t + \mathbf{P} \sin \omega t] \quad (24)$$

Hamiltonian for harmonic oscillator with unit mass and frequency,  $\omega$  is

$$\mathbf{H} = \frac{1}{2}(\mathbf{P}^2 + \omega^2 \mathbf{Q}^2) \quad (25)$$

It is a Hermitian operator that represents the energy of a harmonic oscillator. Making use of (23) solves corresponding energy eigenvalue equation (26).

$$\mathbf{H}|n\rangle = E_n|n\rangle \quad (26)$$

The solution yields energy eigenvalues,  $E_n$  belonging to eigenfunctions  $|n\rangle$ .

$$E_n = \hbar\omega\left(n + \frac{1}{2}\right) \quad (27)$$

Eigenstates of quantized Hamiltonian, (25) having energy eigenvalues, (27) are termed as number states. Since energy eigenvalues of a harmonic oscillator cannot be negative its energy spectrum is positive definite. The lowest eigenstate of the harmonic oscillator is defined as its ground state and corresponds to  $n=0$ . This state is called vacuum state. The creation operator raises the energy and number of quanta in a state, while the annihilation operator lowers them. These operators are, therefore, termed as raising and lowering operators <sup>[11]</sup>.

$$a|n\rangle = \sqrt{n}|n-1\rangle \quad (28)$$

$$a^+|n\rangle = \sqrt{n+1}|n+1\rangle \quad (29)$$

There is no upper bound for energy eigenvalues. However, there exists a lower bound, the ground state energy of the oscillator equal to  $\frac{1}{2}\hbar\omega$ . This represents the energy of vacuum fluctuations in given mode. Energy levels of a harmonic oscillator are equally spaced by an amount  $\hbar\omega$ . Thus energy spectrum of a harmonic oscillator is discontinuous.

In the quantum mechanical treatment of radiation field, a number state,  $|n_k\rangle$  is used to characterize the number of photons in a particular mode of index, k. A number state is the basic quantum state that differs from a classical field. It is defined as eigenstate of number operator. Unlike classical field quantum field has a ground state that is represented by a vacuum state consisting of field fluctuations with no residual energy. A general state of the harmonic oscillator is the linear combination of the number states given by

$$|S\rangle = \sum_{n=0}^{\infty} C_n |n\rangle \quad (30)$$

The numbers states are orthogonal and form a complete set of basis vectors in Hilbert's space. These states can be used to express any state of the oscillator. Further, any number state can be created by repeated application of creation operators on vacuum state.

$$|n\rangle = \frac{a^{+n}}{\sqrt{n!}}|0\rangle \quad (31)$$

The number states have a fixed number of photons but have a random phase i.e. the phase of the corresponding wave form say of electric field is undefined. These states do not form a suitable representation for optical fields where the total number of photons is large. Single photon number states are now available in a few experimental conditions. However, experimental difficulties have prevented the formation of photon number states with more than one photon. These states are of interest for their possible applications in quantum cryptography and quantum information transfer<sup>[12]</sup>. However, these states are useful for representation of intense fields where the number of photons is very less. They have been used as basis for several situations in quantum optics and laser theories. Photon number state generation with a single two level atom in a cavity has been proposed<sup>[13]</sup>.

**The coherent states:** A coherent state is a state of an oscillator having minimum uncertainty product of momentum and position. Coherent states provide a more appropriate basis for the description of electromagnetic field at optical frequencies<sup>[12]</sup>. A coherent state has a high degree of optical coherence and hence the name coherent state. A coherent state has an indefinite number of photons but a more precisely defined phase than the number state. The product of the uncertainty in amplitude and phase for a coherent state is minimum allowed by the uncertainty principle. Hence they are the closest quantum mechanical states to a classical description of electromagnetic field<sup>[8]</sup>. The quantum fluctuations in a coherent state are equal to the zero point fluctuations, which represent the quantum limit to the reduction of noise in a signal. Even an ideal laser operating in a pure coherent state can still have a quantum noise due to these fluctuations. Coherent states are obtained as the solution of a displaced harmonic

oscillator. The ground states of both displaced and undisplaced harmonic oscillators have non-zero energy given by

$$\langle 0|\mathbf{H}|0\rangle = \frac{1}{2}\hbar \quad (32)$$

By subtracting  $\frac{1}{2}\hbar$ , from the Hamiltonian (25)

$$\mathbf{H}' = \frac{1}{2}(P^2 + \omega^2 Q^2 - \hbar) \quad (33)$$

it is possible to make the ground state energy of a displaced oscillator equals zero:

$$\langle 0|\mathbf{H}'|0\rangle = 0 \quad (34)$$

This change of Hamiltonian does not affect the results of this section; it simplifies various expressions. We select the displacement operator

$$U(p, q) = e^{\frac{i(pQ - qP)}{\hbar}} \quad (35)$$

It is a unitary operator that displaces the position,  $Q$  and momentum,  $P$  of any state by  $c$ -numbers  $p$  and  $q$  respectively. The effect of this unitary operator on any operator function of  $P$  and  $Q$  is given by <sup>[15]</sup>.

$$U^{-1}(p, q)(\alpha P + \beta Q)U(p, q) = \alpha(P + p) + \beta(Q + q) \quad (36)$$

And

$$U(p, q)(\alpha P + \beta Q)U^{-1}(p, q) = \alpha(P - p) + \beta(Q - q) \quad (37)$$

Where  $\alpha$  and  $\beta$  are parameters. For a displaced harmonic oscillator,

$$U(p, q)\mathbf{H}'|0\rangle = 0 \quad (38)$$

Where  $U(p, q)$  is the unitary operator defined in (35)

$$U(p, q)\mathbf{H}'U(p, q)^{-1}U(p, q)|0\rangle = 0 \quad (39)$$

And by using (33) and (37).

$$\frac{1}{2}[(P - p)^2 + (Q - q)^2 - \hbar] |p, q\rangle = 0 \quad (40)$$

Where

$$\mathbf{U}(p, q)|0\rangle \equiv |p, q\rangle \quad (41)$$

Eq. (41) represent the ground state of a harmonic oscillator whose coordinate and momentum are displaced by  $p$  and  $q$  respectively. Then for vacuum state where there is no particle to annihilate

$$\mathbf{U}(p, q)\mathbf{a}|0\rangle = 0 \quad (42)$$

And

$$\mathbf{U}(p, q)\mathbf{a}\mathbf{U}^{-1}(p, q)\mathbf{U}(p, q)|0\rangle = 0 \quad (43)$$

Then by using (36) and (37) we can write

$$\mathbf{a}|p, q\rangle = \frac{1}{\sqrt{2\hbar}}(q + ip)|p, q\rangle \quad (44)$$

This is in the form of an eigenvalue equation for the operator  $\mathbf{a}$  in which  $|p, q\rangle$  is the eigenstate having eigenvalue  $\frac{1}{\sqrt{2\hbar}}(q + ip)$ . The eigen value of the adjoint operator

$\frac{1}{\sqrt{2\hbar}}(q - ip)$  corresponding to the adjoint state  $\langle p, q|$ . Based on (44) we can define the

coherent state as eigenstate of the annihilation operator  $\mathbf{a}$  with a complex eigenvalue

$$\alpha = \frac{1}{\sqrt{2\hbar}}(q + ip)$$

$$\mathbf{a}|\alpha\rangle = \alpha|\alpha\rangle \quad (45)$$

$\mathbf{a}$ , being an operator of non-hermitian character its eigenvalues are not restricted to be real but can be imaginary or complex as well. The state of vacuum is a coherent state with eigenvalue zero. Now, the unitary operator defined in (35) can be written in terms of  $\mathbf{a}$  and  $\mathbf{a}^\dagger$

$$\mathbf{U}(\mathbf{p}, \mathbf{q}) = \text{Exp}(\alpha \mathbf{a}^\dagger - \alpha^* \mathbf{a}) \quad (46)$$

Using the Baker-Hausdorff formula and the commutation properties of  $\mathbf{a}$  and  $\mathbf{a}^\dagger$  one can write  $\mathbf{U}(\mathbf{p}, \mathbf{q})$  in more appropriate form

$$\mathbf{U}(\mathbf{p}, \mathbf{q}) = \text{Exp}\left(-\frac{1}{2}|\alpha|^2 + \alpha \mathbf{a}^\dagger - \alpha^* \mathbf{a}\right) \quad (47)$$

Using (45) the coherent states can be written in terms of number states.

$$|\mathbf{p}, \mathbf{q}\rangle = \mathbf{U}(\mathbf{p}, \mathbf{q})|0\rangle = \text{Exp}\left(-\frac{1}{2}|\alpha|^2\right) \sum_{n=0}^{\infty} \frac{\alpha^n \mathbf{a}^{\dagger n}}{n!} |0\rangle \quad (48)$$

And by using (31)

$$|\mathbf{p}, \mathbf{q}\rangle = \text{Exp}\left(-\frac{1}{2}|\alpha|^2\right) \sum_{n=0}^{\infty} \frac{\alpha^n}{n!} |n\rangle = |\alpha\rangle \quad (49)$$

This establishes the connection of coherent state with ground state of a displaced harmonic oscillator. It is customary to replace  $\mathbf{U}(\mathbf{p}, \mathbf{q})$  by  $\mathbf{D}(\alpha)$  while discussing the properties of coherent states. The unitary operator  $\mathbf{D}(\alpha)$  has the following properties.

$$\mathbf{D}^\dagger(\alpha) = \mathbf{D}^{-1}(\alpha) = \mathbf{D}(-\alpha) \quad (50)$$

$$\mathbf{D}^\dagger(\alpha) \mathbf{a} \mathbf{D}(\alpha) = \mathbf{a} + \alpha \quad (51)$$

$$\mathbf{D}^\dagger(\alpha) \mathbf{a}^\dagger \mathbf{D}(\alpha) = \mathbf{a}^\dagger + \alpha^* \quad (52)$$

Using these properties the expressions for various quantities are derived in the next chapter.  $\mathbf{D}(\alpha)$ , operating on vacuum generates a coherent state,  $|\alpha\rangle$ . It is shown to be an eigenstate of annihilation operator as follows.

$$\mathbf{D}^+(\alpha)\mathbf{a}|\alpha\rangle = \mathbf{D}^+(\alpha)\mathbf{a}\mathbf{D}(\alpha)|0\rangle = (\mathbf{a} + \alpha)|0\rangle = \alpha|0\rangle \quad (53)$$

$$\mathbf{D}(\alpha)\mathbf{D}^+(\alpha)\mathbf{a}|\alpha\rangle = \mathbf{D}(\alpha)\alpha|0\rangle = \alpha\mathbf{D}(\alpha)|0\rangle = \alpha|\alpha\rangle \quad (54)$$

Using (31) one can write the scalar product of  $|\alpha\rangle$  with  $|n\rangle$ .

$$\langle n|\alpha\rangle = \frac{\alpha^n}{\sqrt{n!}}\langle 0|\alpha\rangle \quad (55)$$

Expanding  $|\alpha\rangle$  in terms of number state with expansion coefficient  $\langle n|\alpha\rangle$ .

$$|\alpha\rangle = \langle 0|\alpha\rangle \sum_n \frac{\alpha^n}{\sqrt{n!}}|n\rangle \quad (56)$$

$$\langle \alpha| = \langle \alpha|0\rangle^* \sum_n \frac{\alpha^{*n}}{\sqrt{n!}}\langle n| \quad (57)$$

And the norm of the state vector,  $|\alpha\rangle$  is

$$\langle \alpha|\alpha\rangle = |\langle \alpha|0\rangle|^2 e^{|\alpha|^2} = 1 \quad (58)$$

Thus coherent states are normalized. Important properties <sup>[15]</sup> of the coherent states are listed below.

1. Two coherent states  $|\alpha\rangle$  and  $|\alpha'\rangle$  can never be orthogonal for all  $\alpha$  and  $\alpha'$  lying <sup>[13]</sup> in the range  $0 < |\alpha - \alpha'| \leq 1$ . However,  $|\alpha\rangle$  can be approximately orthogonal to  $|0\rangle$  if  $|\alpha| \gg 1$ .
2. Coherent states are the only eigenstates of  $\mathbf{a}$ . One can not similarly constructs the eigen states of creation operator.

3. Probability distribution of photons in a coherent state is a Poisson distribution <sup>[2]</sup>.
4. Coherent states form a two dimensional continuum of states and are, in fact, over complete.

**The Squeezed states:** Squeezed states form a general class of minimum uncertainty states of which coherent states are a particular member with equal noise in both quadratures. Squeezed states <sup>[10]</sup> may have less noise in one quadrature and more noise in the other quadrature than a coherent state to satisfy the requirements of a minimum uncertainty state.

Creation and annihilation operators are written as linear combination of two hermitian operators  $X_1$  and  $X_2$ .

$$\mathbf{a} = \frac{\mathbf{X}_1 + i\mathbf{X}_2}{2} \quad (60)$$

And

$$\mathbf{a}^+ = \frac{\mathbf{X}_1 - i\mathbf{X}_2}{2} \quad (61)$$

They are the real and imaginary parts of complex amplitude that represents the dimensionless amplitudes for the modes of the two-quadrature phases. They follow the commutation relation

$$[\mathbf{X}_1, \mathbf{X}_2] = 2i \quad (62)$$

And the corresponding uncertainty principle is

$$\Delta\mathbf{X}_1\Delta\mathbf{X}_2 \geq 1 \quad (63)$$

Eqn. (63) defines three kinds of states. They are the squeezed states represented by the equality sign, coherent states represented by (64) and other physically probable states, which may not be of minimum uncertainty character

$$\Delta X_1 = \Delta X_2 = 1 \quad (64)$$

A coherent state having equal uncertainties in both quadrature phases may be represented by an error circle in the complex amplitude plane whose axes are  $X_1$  and  $X_2$  (Fig: 2). The center of the error circle lies at

$$\frac{1}{2} \langle X_1 + iX_2 \rangle = \alpha \quad (65)$$

And the radius (64) accounts for the uncertainties in  $X_1$  and  $X_2$ . Squeezed states that correspond to the equality sign in (63) lies on a hyperbola, when  $\Delta X_1$  is plotted against  $\Delta X_2$  (Fig: 3). The points lying to the right of this hyperbola corresponds to physical states that may not be of minimum uncertainty. Squeezed states have reduced uncertainty in one quadrature at the expense of increased uncertainty in the other. While the quantum noise in one quadrature is less than in vacuum, it is more than that in vacuum in the other quadrature. They are represented by the (Fig: 4). The unitary squeeze operator<sup>[14]</sup> that generates squeezed states is

$$S(\varepsilon) = \exp\left(\frac{1}{2}\varepsilon^* a^2 - \frac{1}{2}\varepsilon a^{\dagger 2}\right) \quad (66)$$

, where  $\varepsilon = re^{2i\phi}$  is the complex squeezing parameter. It is expressed in polar coordinates. The amplitude  $r$  is called squeeze factor and  $\phi$ , the half of the argument, is called phase factor. Squeeze operator is a unitary operator with the properties

$$S^+(\varepsilon) = S^{-1}(\varepsilon) = S(-\varepsilon) \quad (67)$$

This operator transforms creation and annihilation operators in the following manner:

$$S^+(\varepsilon)aS(\varepsilon) = a \cosh r - a^{\dagger} e^{-2i\phi} \sinh r \quad (68)$$

$$S^+(\varepsilon)a^{\dagger}S(\varepsilon) = a^{\dagger} \cosh r - a e^{2i\phi} \sinh r \quad (69)$$

Squeezed states find applications in optical communication theory and the interferometric detection of gravitational radiation. By making an optimum choice of phase factor it may be possible to increase the maximum sensitivity <sup>[15]</sup> of the device at lower laser powers. Squeezed states may be produced by several promising methods <sup>[16]</sup> in the field of non-linear optics. Squeezed light has non-classical nature in which characteristic correlations exist between photons. Since they can exist in an interaction free environment, it is possible to store the entanglement of light in them. Squeezed light may be used for super sensitive atomic measurements.

## 2.5. Non-classical properties of light:

Individual photons in non-classical light are strongly correlated. The amount of correlation among individual photons in classical light is limited. Squeezed photons exhibit many non-classical correlations. The light generated in non-linear optical processes like second harmonic generation and parametric down conversion are examples of non-classical light. In the second harmonic generation frequency is doubled inside a special crystal so that red photons are converted to blue photons. In contrast, frequency is divided in parametric down conversion so that blue photons are converted into red photons. The pair wise character of both processes makes them non-classical. Intensity correlation experiments of Hanbury-Brown and Twiss <sup>[17]</sup> that used photon counters and digital correlation are called photon correlation experiments. These experiments measure two-photon correlation function, which is defined as the joint photo count probability of detecting the arrival of a photon at time  $t$  and another photon at time  $t + \tau$ . It is given by

$$G^2(\tau) = \langle E^-(t)E^-(t+\tau)E^+(t+\tau)E^+(t) \rangle = \langle : I(t)I(t+\tau) : \rangle \quad (70)$$

and

$$G^2(\tau) \propto \langle :n(t)n(t+\tau): \rangle \quad (71)$$

The symbol  $: :$  inside the expectation value indicates normal ordering,  $I(t)$  is the intensity of the analogue measurements and  $n(t)$  is the photon number in the photon counting measurements. The normalized form of second order correlation function is

$$g^2(\tau) = \frac{G^2(\tau)}{|G^1(0)|^2} \quad (72)$$

For a field having second-order coherence,  $g^2(\tau)=1$ . If time delay  $\tau=0$ , correlation function for a single mode field <sup>[8]</sup> can be written as follows

$$g^2(0) = 1 + \frac{\int \mathbf{P}(\varepsilon) \left( |\varepsilon|^2 - \langle |\varepsilon|^2 \rangle \right)^2 d^2\varepsilon}{\left( \langle |\varepsilon|^2 \rangle \right)^2} \quad (73)$$

For classical fields the probability distribution  $\mathbf{P}(\varepsilon)$  is positive, hence  $g^2(0) \geq 1$ . Now for the field with a Lorentzian spectrum

$$g^2(\tau) = 1 + e^{-\gamma\tau} \quad (74)$$

And for the field with a Gaussian spectrum

$$g^2(\tau) = 1 + \text{Exp}(-\gamma^2\tau^2) \quad (75)$$

, where  $\gamma$  is the spectral line width. For delay times very large compared to  $\tau_c$ , the correlation time of light, the correlation function factorizes and  $g^2(\tau) \rightarrow 1$ . When  $\tau < \tau_c$ ,  $g^2(0)$  for chaotic light is twice that of coherent light. This is due to the increased intensity fluctuations in the chaotic light field. It is related to the probability that the photon that triggers the counter occurs during a high intensity fluctuation so that the second photon will be detected arbitrarily soon. This effect is called photon bunching

and was first detected by Hanbury-brown and Twiss. This is deduced from a purely classical analysis of the electromagnetic field with fluctuating amplitudes for the modes.

For a quantized electromagnetic field of single mode second order correlation function is given by

$$g^2(0) = \frac{\langle \mathbf{a}^+ \mathbf{a}^+ \mathbf{a} \mathbf{a} \rangle}{\langle \mathbf{a}^+ \mathbf{a} \rangle^2} = 1 + \frac{V(n) - \bar{n}}{\bar{n}^2} \quad (76)$$

Where

$$V(n) = \langle (\mathbf{a}^+ \mathbf{a})^2 \rangle - \langle \mathbf{a}^+ \mathbf{a} \rangle^2 \quad (77)$$

$V(n) = \bar{n}$  for a coherent state and hence,  $g^2(0) = 1$ . It exhibits a Poissonian distribution in the photon number. For a number state  $g^2(0) = 1 - \frac{1}{n}$ ,  $n > 2$ . This is because a number state has zero variance in the photon number. When,  $g^2(\tau) < g^2(0)$  there is a tendency for photons to arrive in pairs. This situation is known as photon bunching. The converse situation in which  $g^2(\tau) > g^2(0)$  is called photon antibunching. The value of  $g^2(0)$  less than unity is not predicted by classical analysis. To get such a value elements of negative probability are required which is forbidden for a true probability distribution. Thus photon antibunching is a feature peculiar to the quantum mechanical nature of electromagnetic field.

Even though photon antibunching and the sub-poissonian statistics are closely related, a close distinction should be maintained between them. We know that for Poissonian statistics the variance of photon number is equal to the mean. The quantity

$$V(n) - \langle n \rangle = Q \quad (78)$$

Provides a measure of sub-poissonian statistics. For a stationary electromagnetic field it may be expressed as follows

$$V(n) - \langle n \rangle = \frac{\langle n \rangle^2}{T^2} \int_{-T}^T d\tau (T - |\tau|) [g^2(\tau) - 1] \quad (79)$$

Where T is the counting time interval. It is obvious that when  $g^2(\tau) = 1$  the field exhibits Poissonian statistics and the field for which  $g^2(\tau) < 1$  for all  $\tau$  will exhibit sub-Poissonian statistics. It is possible to specify the fields that exhibit super-Poissonian statistics for some time interval.

## 2.6. Non-local properties of electromagnetic field:

In the 1960's John Bell showed that a pair of entangled particles, which were once in contact but later move too far apart to interact directly, can exhibit behavior that is too strongly correlated to be explained by classical statistics. These correlations can be explained only by quantum mechanics. Experiments on photons and other particles have confirmed the presence of these correlations, thereby providing strong evidence for the validity of quantum mechanics. These correlations are observed only in the entangled states of the particle and were first discussed in the context of EPR paradox. It may be noted that that the kind of information provided by entanglement of photons cannot deliver a meaningful and controllable message. It was first thought that the only use of information transfer through entanglement was to prove the validity of quantum mechanics. The situation has now changed considerably with the discovery of the phenomenon of quantum teleportation. Quantum teleportation is a novel process that makes information transmission and processing possible by recording it in the quantum state of microscopic systems like polarized photons and atoms. Science fiction writers

suggested the name teleportation to the process of making an object or person disintegrate in one place while a perfect replica appears somewhere else. The general idea of accomplishing teleportation is to scan the original object in a way so as to extract all the information from it, and then transmit this information to a receiving location for constructing the replica. The replica need not be constructed using actual material of the original. The replica will, perhaps, contain atoms of the same kinds and arranged exactly in the same pattern as the original. A teleportation machine would be like a fax machine, which works on two-dimensional documents and produce an approximate facsimile without destroying the original. However, unlike a fax machine, the teleportation machine works on 3-dimensional objects and produces an exact copy of the original using a mechanism that destroys the original. The destruction of the original is a consequence of the Uncertainty principle that forbids any measuring or scanning process that extracts all the information from an atom or other object to make its perfect copy. The more accurately an object is scanned, the more it is disturbed by the scanning process, and ultimately one reaches the point where the original state of the object has been completely disrupted, still without having extracted enough information to make a perfect replica. This is a solid argument against teleportation and explains why the scientists did not take the possibility of teleportation seriously. The study of the Einstein-Podolsky -Rosen effect suggested a means to over come the barrier erected by uncertainty principle. In 1993 an international group of six scientists <sup>[16]</sup> showed that perfect teleportation is possible only if the original is destroyed. In order to perform quantum teleportation of an unknown quantum state from a sender to a receiver there must be a classical communication channel between them. Besides this they must share

quantum entanglement such that each possesses one half of a two-particle entangled state. Sender makes a projective measurement of the unknown state together with his component of the shared entangled state. The result of this measurement is send as classical information over the classical communication channel to the receiver. The receiver uses this information to perform a unitary transformation on his component of the shared entangled state, thereby transforming it into an output state identical to the original unknown quantum state. Since the input state is already destroyed by sender's projective measurement teleportation does not result in "cloning" of a quantum state.

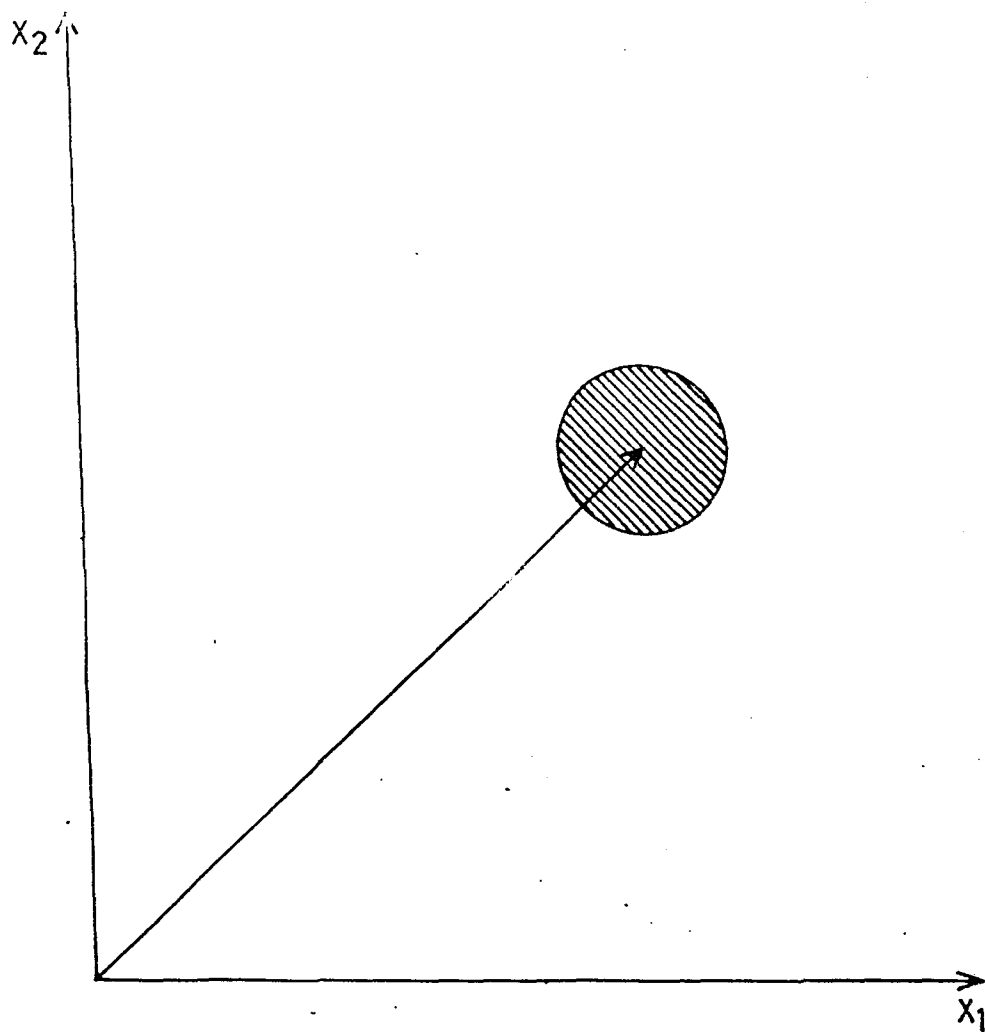


Fig: 2. Phase space plot showing the uncertainty in a coherent state.

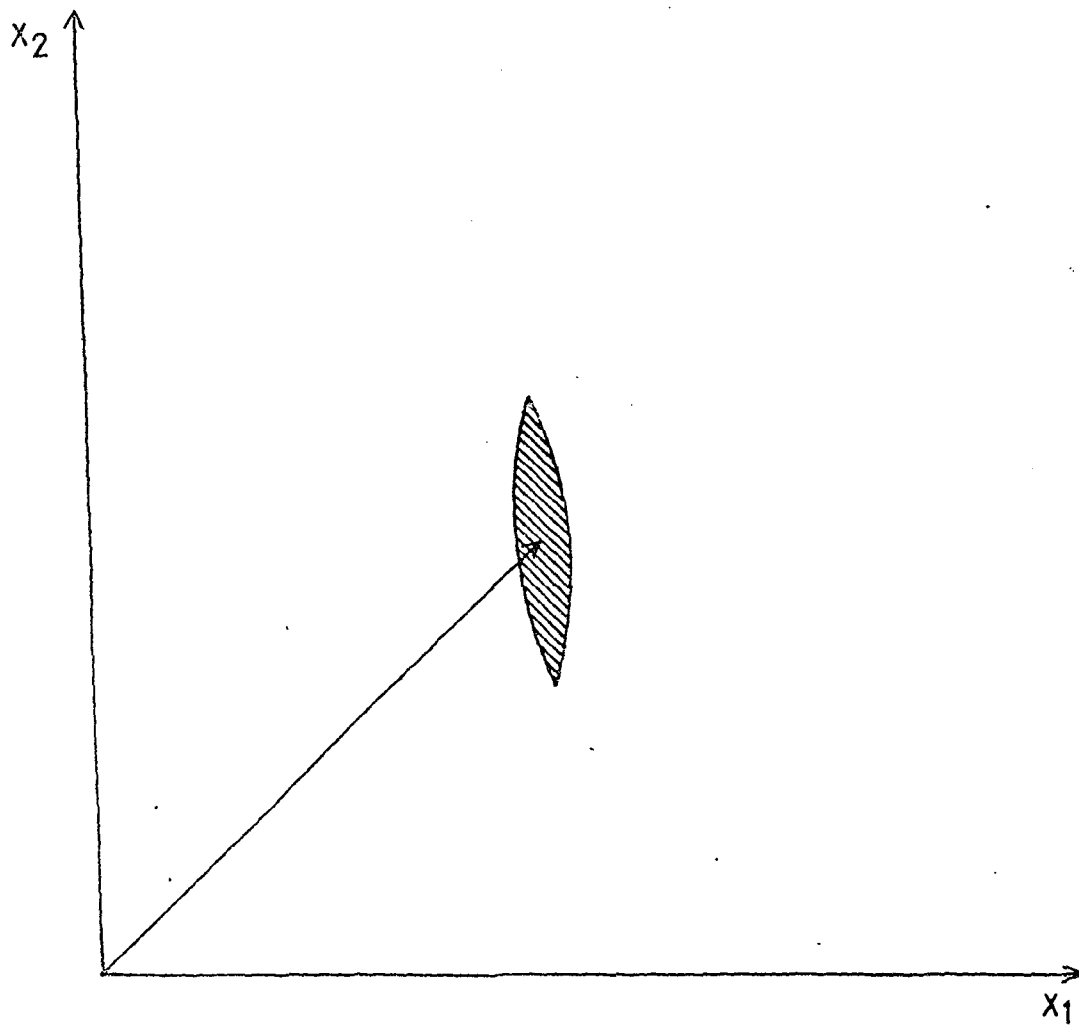


Fig. 3. Phase space plot showing the uncertainty in a squeezed state.

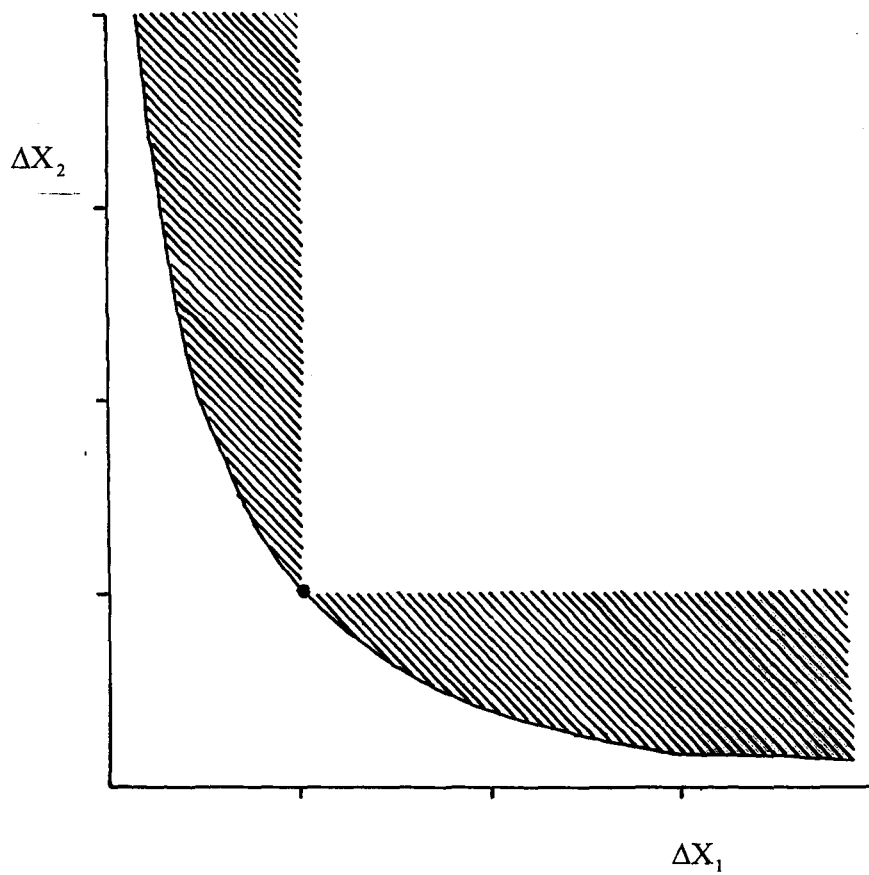


Fig: 4. Plot of  $\Delta X_1$  versus  $\Delta X_2$  for the minimum uncertainty states. The dot marks a coherent state. The shaded region corresponds to the squeezed states.

## Chapter 3

### Properties of states obtained after squeezing and displacing number states

#### 3.1. Introduction:

It is well known that squeezing and displacement operators do not commute. As a result, the states obtained by squeezing a displaced state and by displacing a squeezed state are not identical. The two states obtained by applying these operators to the vacuum state have been studied before. But no study has been made of the states obtained by applying these operators to a number state. The results presented in this chapter fill this gap in our understanding. The two types of states of electromagnetic field are defined as

$$|\varepsilon, \alpha, n\rangle = \mathbf{S}(\varepsilon)\mathbf{D}(\alpha)|n\rangle \quad (1)$$

$$|\alpha, \varepsilon, n\rangle = \mathbf{D}(\alpha)\mathbf{S}(\varepsilon)|n\rangle \quad (2)$$

, where  $\mathbf{D}(\alpha)$  and  $\mathbf{S}(\varepsilon)$  are respectively the time independent squeezing and displacement operators of the free electromagnetic field. The parameters,  $\varepsilon$  and  $\alpha$  are complex quantities. We have calculated the expectation values of the measurable quantities like photon number ( $n$ ), position variable ( $q$ ) and momentum variable ( $p$ ) in these states. The expectation value of the electric field is also obtained in the similar fashion. We have also studied the dependence of these quantities on the amount of squeezing and displacement. This is done to

1. Study the influence of these operators on the values of four variables mentioned above, when they act upon different kind of states.
2. Find out the probable photo count statistics and also the status of minimum uncertainty character of a state, during their operation.

#### 3.2. Popular States of Electromagnetic Field:

The three most popular states of free electromagnetic field are the eigen states of the number operator  $\mathbf{a}^\dagger \mathbf{a}$ , photon annihilation operator  $\mathbf{a}$  and quasi particle annihilation operator  $\mathbf{b}$  obtained as a linear combination of  $\mathbf{a}$  and  $\mathbf{a}^\dagger$  [19]. These states are called number state, coherent state and squeezed state and are denoted by  $|n\rangle, |\alpha\rangle$  and  $|\varepsilon\rangle$  respectively. A number state is produced by repeated application of photon creation operator on the vacuum state

$$|n\rangle = \frac{\mathbf{a}^{\dagger n}}{\sqrt{n!}} |0\rangle \quad (3)$$

, a coherent state  $|\alpha\rangle$  is produced by the action of displacement operator  $\mathbf{D}(\alpha)$  on the vacuum state and a squeezed state  $|\varepsilon\rangle$ , is produced by the action of the squeezing operator,  $\mathbf{S}(\varepsilon)$  on the vacuum state. The squeezing operator squeezes the uncertainty in one quadrature phase at the expense of the uncertainty in the other quadrature phase. Another name of the displaced state and squeezed state is displaced vacuum and squeezed vacuum respectively. The expectation values of the operators  $n$ ,  $p$ ,  $q$  and  $E$  along with their variances  $\Delta n^2, \Delta q^2, \Delta p^2$  and  $\Delta E^2$  for these states are given in table 1. Only the variance of photon number is zero in a number state, but the other variances  $\Delta q^2, \Delta p^2$  and  $\Delta E^2$  are nonzero and related linearly to the photon number  $n$ . Expectation value of the position operator in the displaced vacuum is related to the real part of the complex amplitude,  $\alpha$  and that of the momentum operator to the imaginary part of  $\alpha$ .  $Q$ -value in the number state is always negative and hence it will show only a sub Poissonian distribution.

Table:1  
Expectation values and variances in the basic quantum states of electromagnetic field

Name Of Parameter	$ n\rangle = \frac{\mathbf{a}^{+n}}{(n!)^{\frac{1}{2}}} 0\rangle$	$ \alpha\rangle = \mathbf{D}(\alpha) 0\rangle$	$ \varepsilon\rangle = \mathbf{S}(\varepsilon) 0\rangle$
$\langle n \rangle$	n	$ \alpha ^2$	$\sinh^2 r$
$\langle \Delta n^2 \rangle$	0	$ \alpha ^2$	$2\sinh^2 r \cosh^2 r$
$\langle q \rangle$	0	$\sqrt{\frac{2\hbar}{\omega}} \text{Re}(\alpha)$	0
$\langle \Delta q^2 \rangle$	$\frac{\hbar}{2\omega} (2n+1)$	$\frac{\hbar}{2\omega}$	$\frac{\hbar}{2\omega} \{ \cosh 2r - \sinh 2r \cos 2\phi \}$
$\langle p \rangle$	0	$\sqrt{2\hbar\omega} \text{Im}(\alpha)$	0
$\langle \Delta p^2 \rangle$	$\frac{\hbar\omega}{2} (2n+1)$	$\frac{\hbar\omega}{2}$	$\frac{\hbar\omega}{2} \{ \cosh 2r + \sinh 2r \cos 2\phi \}$
$\langle E \rangle$	0	$-\sqrt{\frac{2\hbar\omega}{\varepsilon_0}} \text{Im}(\gamma)$	0
$\langle \Delta E^2 \rangle$	$\frac{\hbar\omega}{2\varepsilon_0} (2n+1)  u ^2$	$\frac{\hbar\omega}{2\varepsilon_0}  u ^2$	$\frac{\hbar\omega}{2\varepsilon_0} \left\{ \cosh 2r  u ^2 + \sinh 2r [\text{Re}^2 w - \text{Im}^2 w] \right\}$

$U =$  Mode function;  $\gamma = \alpha u e^{-i\alpha t}$ ;  $w = u e^{-i(\omega t + \phi)}$ ;  $\varepsilon = r e^{2i\phi}$ ;  $r = |\varepsilon|$ , squeeze factor;  $\phi =$  Phase

Each coherent state  $|\alpha\rangle$  is a minimum uncertainty state and should show Poissonian distribution. However, in the states obtained by displacing number states and called henceforth excited coherent states may show either super Poisson or sub Poisson distributions depending on the amount of displacement [Fig.5]. The probability

distributions found in the squeezed number states and squeezed vacuum are sub Poissonian for smaller values of  $r$  and if  $r$  is increased then the distributions change to super Poissonian. The value of  $r$  at which changeover occurs depends upon  $n$ . It is depicted for three states in Fig.6 that the plots the  $Q$  value as a function of  $r$ .

A number state is not a minimum uncertainty state in any canonically conjugate observable. However, a squeezed state is a minimum uncertainty state of a set of canonically conjugate variables different from position and momentum but obtained from a linear combination of these operators. The squeezed state becomes a minimum uncertainty state of position and momentum for real squeezing with  $\phi = \pm \frac{n\pi}{2}$ . The

uncertainty product in the state  $|\varepsilon\rangle$  in units of  $\frac{\hbar}{2}$  is plotted in Fig. 7(a) against the phase angle for three different values of Squeezing factor,  $r = 0.1, 0.2$  and  $0.3$ . The uncertainty product in the states obtained by squeezing the number states with  $n = 0, 1$  and  $2$  is plotted in against phase angle Fig. 7(b) for  $r = 0.2$ . It is seen that a state obtained by squeezing a number state, called excited squeezed state, is not a minimum uncertainty state. The Fig: 7(a) further demonstrates that the uncertainty product in the squeezed vacuum becomes minimum at regular intervals of phase angles for any amount of squeezing.

### 3.3. States obtained by squeezing and displacing number states:

The excited displaced states  $|\alpha, n\rangle$  and excited squeezed states  $|\varepsilon, n\rangle$  results from the action of  $\mathbf{D}(\alpha)$  and  $\mathbf{S}(\varepsilon)$  on the number state  $|n\rangle$ . The calculated results of the expectation values of the various operators are given in Table 2.

Table:2  
Expectation values in the displaced and squeezed number states

Name Of Parameter	$D(\alpha) n\rangle =  \alpha, n\rangle$	$S(\varepsilon) n\rangle =  \varepsilon, n\rangle$
$\langle n \rangle$	$n +  \alpha ^2$	$n \cosh 2r + \sinh^2 r$
$\langle \Delta n^2 \rangle$	$(2n + 1) \alpha ^2$	$2 \sinh^2 r \cosh^2 r (n^2 + n + 1)$
$\langle q \rangle$	$\sqrt{\frac{2\hbar}{\omega}} \text{Re}(\alpha)$	0
$\langle \Delta q^2 \rangle$	$\frac{\hbar}{2\omega} (2n + 1)$	$\frac{\hbar}{2\omega} (2n + 1) \{ \cosh 2r - \sinh 2r \cos 2\phi \}$
$\langle p \rangle$	$\sqrt{2\hbar\omega} \text{Im}(\alpha)$	0
$\langle \Delta p^2 \rangle$	$\frac{\hbar\omega}{2} (2n + 1)$	$\frac{\hbar\omega}{2} (2n + 1) \{ \cosh 2r + \sinh 2r \cos 2\phi \}$
$\langle E \rangle$	$-\sqrt{\frac{2\hbar\omega}{\varepsilon_0}} \text{Im}(\gamma)$	0
$\langle \Delta E^2 \rangle$	$\frac{\hbar\omega}{2\varepsilon_0} (2n + 1)  u ^2$	$\frac{\hbar\omega}{2\varepsilon_0} (2n + 1) \left\{ \cosh 2r  u ^2 + \sinh 2r [\text{Re}^2 w - \text{Im}^2 w] \right\}$

U = Mode function;  $\gamma = \alpha u e^{-i\alpha}$ ;  $w = u e^{-i(\alpha + \phi)}$ ;  $\varepsilon = r e^{2i\phi}$ ;  $r = |\varepsilon|$  = squeezing factor ;  $\phi$  = Phase factor

In the displaced number state while the photon number increases by an amount  $|\alpha|^2$ , its variance becomes a linear function of  $n$ . In squeezed number state the photon number is observed to have a hyperbolic dependence on the squeezing factor  $r$  and a linear dependence on  $n$ . Average position and momentum remains zero in the squeezed number state while it is displaced by a factor related to real and imaginary part of complex amplitude  $\alpha$  respectively in the displaced number state. This shows that the only action of displacement operator is to change the average position and momentum and the effect is the same on all the ground and excited states. The variances of position and momentum do not change in the displaced states. In contrast, the squeezing operator does not affect the average values of position and momentum but changes the variances by the same amount in ground and excited states. Thus the effect of displacement operator is opposite to the effect of squeezing operator on the average values of position and momentum and their variance. The displacement operator  $\mathbf{D}(\alpha)$  alters the average value of electric field in the number state but not its variance. The squeezing operator  $\mathbf{S}(\epsilon)$  changes the variance of electric field by a factor multiplied by  $(2n+1)$ .

#### **3.4. Squeezed and displaced states of electromagnetic field:**

The calculated expectation values and variances of various operators in the states resulting from the action of squeezing followed by the displacement and vice-versa are given in Table 3. The order in which displacement and squeezing operators is applied affect the expectation values of photon number, electric field and variance of photon number. However, the variance of electric field remains the same in both orders of application of the two operators. It is also true for the states obtained from excited state

Table:3  
Expectation values in squeezed –displaced state and displaced-squeezed state

Name Of Parameter	$S(\varepsilon)D(\alpha) 0\rangle =  \varepsilon, \alpha\rangle$	$D(\alpha)S(\varepsilon) 0\rangle =  \alpha, \varepsilon\rangle$
$\langle q \rangle$	$ \alpha ^2 \cosh 2r + \sinh^2 2r - \sinh 2r \operatorname{Re}(\chi)$	$\sinh^2 r +  \alpha ^2$
$\langle \Delta n^2 \rangle$	$ \alpha ^2 \cosh^2 2r - \sinh 4r \operatorname{Re}(\chi) + \frac{1}{2} \sinh^2 2r [1 + 2 \alpha ^2]$	$2\sinh^2 r \cosh^2 r +  \alpha ^2 \cosh 2r - \sinh 2r \operatorname{Re}(\chi)$
$\langle q \rangle$	$\sqrt{\frac{2\hbar}{\omega}} (\operatorname{Re}(\alpha) \cosh r - \operatorname{Re}(\eta) \sinh r)$	$\sqrt{\frac{2\hbar}{\omega}} \operatorname{Re}(\alpha)$
$\langle \Delta q^2 \rangle$	$\frac{\hbar}{2\omega} \{ \cosh 2r - \sinh 2r \cos 2\phi \}$	$\frac{\hbar}{2\omega} \{ \cosh 2r - \sinh 2r \cos 2\phi \}$
$\langle p \rangle$	$\sqrt{2\hbar\omega} \{ \cosh r \operatorname{Im}(\alpha) + \sinh r \operatorname{Im}(\eta) \}$	$\sqrt{2\hbar\omega} \operatorname{Im}(\alpha)$
$\langle \Delta p^2 \rangle$	$\frac{\hbar\omega}{2} \{ \cosh 2r + \sinh 2r \cos 2\phi \}$	$\frac{\hbar\omega}{2} \{ \cosh 2r + \sinh 2r \cos 2\phi \}$
$\langle E \rangle$	$-\sqrt{\frac{2\hbar\omega}{\varepsilon_0}} \{ \operatorname{Im}(\gamma) \cosh r + \sinh r \operatorname{Im}(z) \}$	$-\sqrt{\frac{2\hbar\omega}{\varepsilon_0}} \operatorname{Im}(\gamma)$
$\langle \Delta E^2 \rangle$	$\frac{\hbar\omega}{2\varepsilon_0} \left\{ \cosh 2r  u ^2 + \sinh 2r [\operatorname{Re}^2 w - \operatorname{Im}^2 w] \right\}$	$\frac{\hbar\omega}{2\varepsilon_0} \left\{ \cosh 2r  u ^2 + \sinh 2r [\operatorname{Re}^2 w - \operatorname{Im}^2 w] \right\}$

U = Mode function;  $\gamma = \alpha u e^{-i\alpha x}$ ;  $w = u e^{-i(\alpha x + \phi)}$ ;  $\varepsilon = r e^{2i\phi}$ ;  $r = |\varepsilon|$ , squeeze factor ;  $\phi =$  Phase factor  
 $\eta = \alpha \varepsilon^{2i\phi}$ ;  $\chi = \alpha^2 e^{2i\phi}$ ;  $Z = \alpha u^* e^{i(2\phi + \alpha x)}$

Table 4

Name Of Parameter	$S(\varepsilon)D(\alpha) n\rangle =  \varepsilon, \alpha, n\rangle$	$D(\alpha)S(\varepsilon) n\rangle =  \alpha, \varepsilon, n\rangle$
$\langle n \rangle$	$\left\{n +  \alpha ^2\right\} \cosh 2r + \sinh^2 r - \sinh 2r \operatorname{Re}(\chi)$	$n \cosh 2r + \sinh^2 r +  \alpha ^2$
$\langle \Delta n^2 \rangle$	$(2n+1) \left[  \alpha ^2 \cosh^2 2r - \sinh 4r \operatorname{Re}(\chi) \right] + \frac{1}{2} \sinh^2 2r \left[ n^2 + n + 1 + 2(2n+1)  \alpha ^2 \right]$	$2 \sinh^2 r \cosh^2 r (n^2 + n + 1) + (2n+1) \left[  \alpha ^2 \cosh 2r - \sinh 2r \operatorname{Re}(\chi) \right]$
$\langle q \rangle$	$\sqrt{\frac{2\hbar}{\omega}} \{ \operatorname{Re}(\alpha) \cosh r - \operatorname{Re}(\eta) \sinh r \}$	$\sqrt{\frac{2\hbar}{\omega}} \operatorname{Re}(\alpha)$
$\langle \Delta q^2 \rangle$	$\frac{\hbar}{2\omega} (2n+1) [\cosh 2r - \sinh 2r \cos 2\phi]$	$\frac{\hbar}{2\omega} (2n+1) [\cosh 2r - \sinh 2r \cos 2\phi]$
$\langle p \rangle$	$\sqrt{2\hbar\omega} \{ \operatorname{Im}(\alpha) \cosh r + \operatorname{Im}(\eta) \sinh r \}$	$\sqrt{2\hbar\omega} \operatorname{Im}(\alpha)$
$\langle \Delta p^2 \rangle$	$\frac{\hbar\omega}{2} (2n+1) \{ \cosh 2r + \sinh 2r \cos 2\phi \}$	$\frac{\hbar\omega}{2} (2n+1) \{ \cosh 2r + \sinh 2r \cos 2\phi \}$
$\langle E \rangle$	$-\sqrt{\frac{2\hbar\omega}{\varepsilon_0}} \{ \operatorname{Im}(\gamma) \cosh r + \operatorname{Im}(z) \sinh r \}$	$-\sqrt{\frac{2\hbar\omega}{\varepsilon_0}} \operatorname{Im}(\gamma)$
$\langle \Delta E^2 \rangle$	$\frac{\hbar\omega}{2\varepsilon_0} (2n+1) \left\{ \cosh 2r  u ^2 + \sinh 2r [\operatorname{Re}^2 w - \operatorname{Im}^2 w] \right\}$	$\frac{\hbar\omega}{2\varepsilon_0} (2n+1) \left\{ \cosh 2r  u ^2 + \sinh 2r [\operatorname{Re}^2 w - \operatorname{Im}^2 w] \right\}$

U = Mode function;  $\gamma = \alpha u e^{-i\alpha x}$ ;  $w = u e^{-i(\alpha x + \phi)}$ ;  $\varepsilon = r e^{2i\phi}$ ;  $r = |\varepsilon|$  = squeeze factor;  $\phi$  = Phase factor  $\eta = \alpha e^{2i\phi}$ ;  $\chi = \alpha^2 e^{2i\phi}$ ;  $Z = \alpha u^* e^{i(2\phi + \alpha x)}$

,mentioned in eqn. (1) and (2). The general results for any number state of electromagnetic field are given in Table 4.

### 3.5. Some General Comments about the Expectation Values:

We have calculated expectation values and variances of measurable quantities in nine different types of states of electromagnetic field. The 72 results obtained in these states reveals certain general trends regarding the effect of the operators  $\mathbf{D}(\alpha)$  and  $\mathbf{S}(\varepsilon)$  on a given kind of state. It is to be emphasized that the results for a general state given in table4 are new results and all other results given in other tables are obtainable from it by putting the value zero to parameters  $\alpha$ ,  $r$  and  $n$ . Some of the results for the zero values of the parameters were calculated in the past <sup>[7,8]</sup> and agree with the results obtained from table 4.

The expectation value of the number operator measures the energy of a state. The energy in both the states  $|\varepsilon, \alpha, n\rangle$  and  $|\alpha, \varepsilon, n\rangle$  is different from the energy in the state  $|n\rangle$ . Further, the states  $|\varepsilon, \alpha, n\rangle$  and  $|\alpha, \varepsilon, n\rangle$  do not have the same energy. It is possible to express the expectation value of the number operator in general states in terms of the expectation value of the corresponding squeezed number state,  $|\varepsilon, n\rangle$ . Thus,  $\langle n \rangle$  in the state  $|\varepsilon, \alpha, n\rangle$  is given by

$$\langle n \rangle = \langle n \rangle_{|\varepsilon, n\rangle} + |\alpha|^2 \cosh 2r - \sinh 2r \operatorname{Re}(\chi) \quad (4)$$

, while  $\langle n \rangle$  in the state  $|\alpha, \varepsilon, n\rangle$  is given by

$$\langle n \rangle = \langle n \rangle_{|\varepsilon, n\rangle} + |\alpha|^2 \quad (5)$$

Since  $|\alpha|^2$  is a positive definite quantity, the energy content of  $|\alpha, \varepsilon, n\rangle$  is always more than that of  $|\varepsilon, n\rangle$ , which is not true for  $|\varepsilon, \alpha, n\rangle$  due to the dependence of extra term on squeezing factor,  $r$ . The role of  $\mathbf{D}(\alpha)$  and  $\mathbf{S}(\varepsilon)$  in controlling the energy content is observed to be reversed in the above states. This again establishes the fact that order of application of squeezing and displacement operators are very crucial from the point of view of energy.

The variance of photon number in the general states is the sum of three terms. Two terms are the variances in the states  $|\varepsilon, n\rangle$  and  $|\alpha, n\rangle$ , while the third term gives the dependence on the squeeze factor. The variance in the state  $|\varepsilon, \alpha, n\rangle$  is given by

$$\langle \Delta n^2 \rangle = \langle \Delta n^2 \rangle_{|\alpha, n\rangle} + \langle \Delta n^2 \rangle_{|\varepsilon, n\rangle} + (2n+1) \sinh 4r \left\{ |\alpha|^2 \tanh 2r - \text{Re}(\chi) \right\} \quad (6)$$

Similarly, the variance in the state  $|\alpha, \varepsilon, n\rangle$  is given by

$$\langle \Delta n^2 \rangle = \langle \Delta n^2 \rangle_{|\alpha, n\rangle} + \langle \Delta n^2 \rangle_{|\varepsilon, n\rangle} + (2n+1) \sinh 2r \left\{ |\alpha|^2 \tanh r - \text{Re}(\chi) \right\} \quad (7)$$

By putting  $n=0$  in eqs. (6) and (7), one obtains the expansions for the variance in the states  $|\alpha, \varepsilon\rangle$  and  $|\varepsilon, \alpha\rangle$ . The variance in the state  $|\varepsilon, \alpha\rangle$  is given by

$$\langle \Delta n^2 \rangle = \langle \Delta n^2 \rangle_{|\alpha\rangle} + \langle \Delta n^2 \rangle_{|\varepsilon\rangle} + \sinh 4r \left\{ |\alpha|^2 \tanh 2r - \text{Re}(\chi) \right\} \quad (8)$$

and in the state  $|\alpha, \varepsilon\rangle$  by

$$\langle \Delta n^2 \rangle = \langle \Delta n^2 \rangle_{|\alpha\rangle} + \langle \Delta n^2 \rangle_{|\varepsilon\rangle} + \sinh 2r \left\{ |\alpha|^2 \tanh r - \text{Re}(\chi) \right\} \quad (9)$$

We again observe that the variance of photon number in squeezed and displaced vacuum states contains three terms- the first two terms are the variances in displaced and squeezed vacuum and the third term differ gives the dependence on squeeze factor.

It is possible to make similar inferences about the effect of displacement and squeezing operators on the expectation values of position and momentum. The expectation value of the position operator in a state remains unaffected by the action of squeezing operator  $S$

( $\epsilon$ ). However, it is altered by the amount  $\sqrt{\frac{2\hbar}{\omega}}\text{Re}(\alpha)$  when displacement operator  $D(\alpha)$

acts on ground and excited states. Squeezing does make an effect in the displaced state.

The squeezing operator alters the position by the amount  $\sqrt{\frac{2\hbar}{\omega}}\{\text{Re}(\alpha)\cosh r - \text{Re}(\eta)\sinh r\}$  in any number state. It is to be noted that the expectation value of the position in  $|\epsilon, \alpha\rangle$  is same as that in  $|\epsilon, \alpha, n\rangle$ . Action of displacement operator does not alter the variance of position operator. The variances in different states are related in the following manner:

$$\langle \Delta q^2 \rangle_{|\alpha\rangle} = \frac{\hbar}{2\omega} = \langle \Delta q^2 \rangle_{|0\rangle} \quad (10)$$

$$\langle \Delta q^2 \rangle_{|\alpha, n\rangle} = \frac{\hbar}{2\omega} (2n + 1) = \langle \Delta q^2 \rangle_{|n\rangle} \quad (11)$$

$$\langle \Delta q^2 \rangle_{|\epsilon\rangle} = \frac{\hbar}{2\omega} \{\cosh 2r - \sinh 2r \cos 2\phi\} = \langle \Delta q^2 \rangle_{|\alpha, \epsilon\rangle} \quad (12)$$

$$\langle \Delta q^2 \rangle_{|\epsilon, \alpha, n\rangle} = \frac{\hbar}{2\omega} (2n + 1) \{\cosh 2r - \sinh 2r \cos 2\phi\} = \langle \Delta q^2 \rangle_{|\alpha, \epsilon, n\rangle} \quad (13)$$

We infer from the above equations that squeezing changes the variance of position by the factor  $\cosh 2r - \sinh 2r \cos 2\phi$ . This is true for other types of state as well. The results for other states are given below:

$$\langle \Delta q^2 \rangle_{|\epsilon, \alpha, n\rangle} = (\cosh 2r - \sinh 2r \cos 2\phi) \langle \Delta q^2 \rangle_{|\alpha, n\rangle} \quad (14)$$

$$\langle \Delta q^2 \rangle_{|\epsilon, n\rangle} = (\cosh 2r - \sinh 2r \cos 2\phi) \langle \Delta q^2 \rangle_{|n\rangle} \quad (15)$$

$$\langle \Delta q^2 \rangle_{|\varepsilon, \alpha\rangle} = (\cosh 2r - \sinh 2r \cos 2\phi) \langle \Delta q^2 \rangle_{|\alpha\rangle} \quad (16)$$

$$\langle \Delta q^2 \rangle_{|\varepsilon, \alpha\rangle} = \frac{\hbar}{2\omega} \{\cosh 2r - \sinh 2r \cos 2\phi\} = \langle \Delta q^2 \rangle_{|\alpha, \varepsilon\rangle} \quad (17)$$

The variance of position operator remains the same if the order in which  $\mathbf{D}(\alpha)$  and  $\mathbf{S}(\varepsilon)$  are applied on a number state is reversed as shown by Eqs. (13), and (17) above.

Similar conclusions are drawn about the momentum operator. Squeezing a number state does not alter the expectation value of the momentum operator. Displacement operator alters the momentum of any kind of number state. As in the case of position operator we note that squeezing changes the momentum of a number state which has already been displaced. It is also noted that action of squeezing do not distinguish between the ground and excited state if it has already been displaced.

$$\langle \mathbf{p} \rangle_{|\varepsilon, \alpha, n\rangle} = \langle \mathbf{p} \rangle_{|\varepsilon, \alpha\rangle} \quad (18)$$

In order to change the momentum in a given state, the effective way is to displace it rather than to squeeze it. The squeezing is, however, effective in displaced ground and excited states.

Variance of momentum is not altered when a given state is displaced

$$\langle \Delta p^2 \rangle_{|\alpha, n\rangle} = \frac{\hbar\omega}{2} (2n + 1) = \langle \Delta p^2 \rangle_{|n\rangle} \quad (19)$$

$$\langle \Delta p^2 \rangle_{|\alpha\rangle} = \frac{\hbar\omega}{2} = \langle \Delta p^2 \rangle_{|0\rangle} \quad (20)$$

$$\langle \Delta p^2 \rangle_{|\alpha, \varepsilon\rangle} = \frac{\hbar\omega}{2} \{\cosh 2r + \sinh 2r \cos 2\phi\} = \langle \Delta p^2 \rangle_{|\varepsilon\rangle} \quad (21)$$

$$\langle \Delta p^2 \rangle_{|\alpha, \epsilon, n\rangle} = \frac{\hbar\omega}{2} (2n+1) \{ \cosh 2r + \sinh 2r \cos 2\phi \} = \langle \Delta p^2 \rangle_{|\epsilon, \alpha, n\rangle} \quad (22)$$

Only squeezing can change the variance of momentum and the change is by a factor  $\cosh 2r + \sinh 2r \cos 2\phi$  independent of the type of state, which is squeezed.

$$\langle \Delta p^2 \rangle_{|\epsilon, \alpha, n\rangle} = (\cosh 2r + \sinh 2r \cos 2\phi) \langle \Delta p^2 \rangle_{|\alpha, n\rangle} \quad (23)$$

$$\langle \Delta p^2 \rangle_{|\epsilon, n\rangle} = (\cosh 2r + \sinh 2r \cos 2\phi) \langle \Delta p^2 \rangle_{|n\rangle} \quad (24)$$

$$\langle \Delta p^2 \rangle_{|\epsilon, \alpha\rangle} = (\cosh 2r + \sinh 2r \cos 2\phi) \langle \Delta p^2 \rangle_{|\alpha\rangle} \quad (25)$$

$$\langle \Delta p^2 \rangle_{|\alpha, \epsilon\rangle} = \frac{\hbar\omega}{2} \{ \cosh 2r + \sinh 2r \cos 2\phi \} = \langle \Delta p^2 \rangle_{|\epsilon, \alpha\rangle} \quad (26)$$

Variance of momentum remains the same if the order in which  $\mathbf{D}(\alpha)$  and  $\mathbf{S}(\epsilon)$  applied on a number state are reversed as shown in Eqs. (22) and (26).

The expectation value of the electric field operator is zero in a number state but varies in a sinusoidal fashion in a displaced number state. Squeezing a number state does not affect the expectation value of the electric field. The expectation value of the electric field in a state depends on the order in which operators  $\mathbf{D}(\alpha)$  and  $\mathbf{S}(\epsilon)$  act upon it and does not depend upon the number of photons. The variance of electric field depends linearly upon photon number in the number state of any kind. Squeezing changes the variance by a fixed factor  $\cosh 2r |u|^2 + \sinh 2r [\text{Re}^2 w - \text{Im}^2 w]$  in all states. Displacement has no effect on the variance of the electric field in a state. The variance electric field does not depend upon the order in which  $\mathbf{D}(\alpha)$  and  $\mathbf{S}(\epsilon)$  are applied on a number state. All these results are depicted algebraically by the following equations:

$$\langle \Delta E^2 \rangle_{|\alpha, \epsilon\rangle} = \frac{\hbar\omega}{2\epsilon_0} \{ \cosh 2r |u|^2 + \sinh 2r [\text{Re}^2 w - \text{Im}^2 w] \} = \langle \Delta E^2 \rangle_{|\epsilon, \alpha\rangle} \quad (27)$$

$$\langle \Delta E^2 \rangle_{|\alpha, \varepsilon, n\rangle} = \frac{\hbar\omega}{2\varepsilon_0} \left\{ \cosh 2r |u|^2 + \sinh 2r [\operatorname{Re}^2 w - \operatorname{Im}^2 w] \right\} = \langle \Delta E^2 \rangle_{|\varepsilon, \alpha, n\rangle} \quad (28)$$

### 3.5. Minimum Uncertainty Character of the States:

The uncertainty product of the position and momentum and the Q values are calculated for all the above noted nine types of states. The uncertainty product allows us to investigate the minimum uncertainty character while the Q value allows us to infer the nature of photo count statistics. The results are given in Table 5. Among the basic states only coherent state is of minimum uncertainty. A squeezed state is not a minimum uncertainty state of momentum and position; it is a minimum uncertainty state of another set of canonically conjugate operators that are linear combination of the position and momentum operators. The state  $|\varepsilon, \alpha\rangle$  may be cited as an example. Squeezing an undisplaced vacuum enhances its uncertainty product in general. However, if the phase factor  $\phi = \pm \frac{n\pi}{2}$ , where n is an integer, one obtains a state of minimum uncertainty. We

can summaries the results on the uncertainty product as:

1. Excited states of any kind are not minimum uncertainty states.
2. Squeezing enhances the uncertainty product beyond minimum unless  $\phi = \pm \frac{n\pi}{2}$ .

Table 5

Name Of states	$\Delta p \Delta q$	$Q = \langle \Delta n \rangle^2 - \langle n \rangle$	P.C.S
$ n\rangle$	$\frac{\hbar}{2}(2n+1)$	$-n$	Sub Poissonian
$ \alpha\rangle$	$\frac{\hbar}{2}$	0	Poissonian
$ \varepsilon\rangle$	$\frac{\hbar}{2}(\cosh^2 2r - \sinh^2 2r \cos^2 2\phi)^{\frac{1}{2}}$	$\sinh^2 r \cosh 2r$	Super Poissonian
$ \alpha, n\rangle$	$\frac{\hbar}{2}(2n+1)$	$n(2 \alpha ^2 - 1)$	Super Poissonian
$ \varepsilon, n\rangle$	$\frac{\hbar}{2}(2n+1) \left( \begin{array}{c} \cosh^2 2r \\ -\sinh^2 2r \cos^2 2\phi \end{array} \right)^{\frac{1}{2}}$	$\cosh 2r(\sinh^2 r - n) + 2n(n+1)\sinh^2 r \cosh^2 r$	Sub Poissonian Poissonian Super Poissonian
$ \varepsilon, \alpha\rangle$	$\frac{\hbar}{2}(\cosh^2 2r - \sinh^2 2r \cos^2 2\phi)^{\frac{1}{2}}$	$\sinh^2 r \cosh 2r(1 + 2 \alpha ^2) +  \alpha ^2 \sinh^2 2r - 2\sinh^2 r \sinh 2r \operatorname{Re}(\chi)$	Sub Poissonian Poissonian Super Poissonian
$ \alpha, \varepsilon\rangle$	$\frac{\hbar}{2}(\cosh^2 2r - \sinh^2 2r \cos^2 2\phi)^{\frac{1}{2}}$	$\sinh^2 r \left\{ \cosh 2r + 2 \alpha ^2 - \sinh 2r \operatorname{Re}(\chi) \right\}$	do
$ \varepsilon, \alpha, n\rangle$	$\frac{\hbar}{2}(2n+1) \left( \begin{array}{c} \cosh^2 2r \\ -\sinh^2 2r \cos^2 2\phi \end{array} \right)^{\frac{1}{2}}$	$(2n+1) \left[ \begin{array}{c}  \alpha ^2 \cosh^2 2r \\ -\sinh 4r \operatorname{Re}(\chi) \end{array} \right] + 2\sinh^2 r \cosh^2 r \left[ \begin{array}{c} n^2 + n + 1 \\ + 2(2n+1) \alpha ^2 \end{array} \right] - \cosh 2r(n +  \alpha ^2) - \sinh^2 r + \sinh 2r \operatorname{Re}(\chi)$	do
$ \varepsilon, \alpha, n\rangle$	$\frac{\hbar}{2}(2n+1) \left( \begin{array}{c} \cosh^2 2r \\ -\sinh^2 2r \cos^2 2\phi \end{array} \right)^{\frac{1}{2}}$	$2\sinh^2 r \cosh^2 r(n^2 + n + 1) + (2n+1) \left[ \begin{array}{c}  \alpha ^2 \cosh 2r \\ -\sinh 2r \operatorname{Re}(\chi) \end{array} \right] - n \cosh 2r - \sinh^2 r -  \alpha ^2$	do

### 3.7. Photo Count Distributions of Different States:

Photo count distributions measured in some spontaneous Biophoton signals appears to be mainly Poissonian. There are a few signals whose photo count statistics appear to be sub or super Poissonian. The possibility of the existence of sub, super or simply Poissonian statistics mitigates against any semi-classical description of biophoton emission. The results given in Table 5 indicate that pure quantum states can show such statistics. A simple indicator of the type of statistics is provided by the Q-value

$$Q = \langle \Delta n^2 \rangle - \langle n \rangle . \quad (29)$$

the Q- value in a given quantum state gives the nature of photo count distributions of the electromagnetic field in this state. The values  $Q = 0$ ,  $Q < 0$  and  $Q > 0$ , give Poisson, sub Poisson and super Poisson distributions respectively. Q-values are calculated for all states studied by us. The dependence of the Q-value on four parameters i.e., squeezing factor ( $r$ ), Phase angle ( $\phi$ ), photon number ( $n$ ) and  $\alpha$  are studied by us. The dependence of the Q-value on phase angle and squeezing factor in two general states of electromagnetic field  $|\alpha, \varepsilon, n\rangle$  and  $|\varepsilon, \alpha, n\rangle$  is presented in greater detail. The Fig. 8 and 9 give the results for the state  $|\varepsilon, \alpha, n\rangle$  and Fig. 14 and 15 gives the results for the state  $|\alpha, \varepsilon, n\rangle$ . These figures demonstrate that both states can exhibit super Poissonian statistics at higher displacement and squeezing levels for any value of photon number. Both states can show sub Poisson distribution at very low displacement for a range of values of squeezing factor,  $r$  at selected phase angle irrespective of the photon number. The selected phase angles include zero radian. It is depicted in Fig.10 and 16. When the displaced vacuum is squeezed Q-value varies with respect to phase angle in a sinusoidal fashion at all values

of squeezing factor; the value continuously changes from positive to negative and back to positive. The variation implies that the distribution changes from sub Poissonian to super Poissonian regimes for small values of  $r$  as depicted in the Fig: 17. The  $Q$ -value becomes positive definite for  $r$  greater than 0.316. The value of  $r$  at the transition point increases with the  $|\alpha|^2$ . This means that one cannot get sub Poissonian statistics at higher squeezing levels from a displaced vacuum state.  $Q$ -value is plotted against the phase angle for a coherent state with  $|\alpha|^2 = .5$  for different values of squeezing factor  $r = .1, .2, .4$  in this figure. The behavior of  $Q$ -values is similar in the states obtained by squeezing the displaced number state.  $Q$ -value of  $n=2$  displaced number state with  $|\alpha|^2 = .5$  is plotted against the phase angle in Fig. 18. The sinusoidal variation of  $Q$ -value with phase angle between a negative minimum and positive maximum is a common observation in  $|\varepsilon, \alpha, n\rangle$  states. However, the variation will be restricted to positive values at higher levels of squeezing and displacement. The photo count distribution will be sub Poissonian for small values of  $r$  and  $|\alpha|^2$  for all number states. In order to confirm this  $Q$ -values are again plotted against phase angle for three sets of values for  $r$  and  $|\alpha|^2$  in Fig. 19.

A squeezed vacuum will show a photo count distribution of super Poissonian nature for any value of squeezing factor. When such a state is displaced  $Q$ -value shows an oscillatory behavior with respect to phase angle. The minimum of the  $Q$  value is negative and its maximum is positive, which implies that both sub and super Poissonian distributions can occur. It is indicated in Fig.11. The amplitude of this oscillation decreases with the increase in the value of  $|\alpha|^2$  in the displaced and squeezed vacuum

state. Thus such a state can show both sub and super Poisson distributions for any amount of displacement. This behaviour occurs only for small values of  $r$ . At higher squeezing levels the oscillations do occur but are limited to super Poissonian regime. In order to elucidate this behaviour we have plotted  $Q$ -value as a function of phase angle at three sets of values in Fig. 20. The phase angle dependence of  $Q$ -value in the excited states is similar to that in the ground state, though the minimum of  $Q$ -value lies in the super Poissonian region. The  $Q$ -value as a function of phase angle is plotted for a displaced  $n=1$  state in Fig. 12 and for displaced  $n=2$  state in Fig.13. The  $Q$ -value of the corresponding squeezed number state is kept to a low positive value by adjusting the value of  $r$  and the plots are made at these values of  $r$ . From these plots, we conclude that the state  $|\alpha, \varepsilon\rangle$  is bound to exhibit super Poissonian statistics at large values of  $r$ . But the distribution of corresponding excited state will be super Poissonian except at very low values of  $r$ .

The statistical distributions of various types of states suggest that squeezed states appear to be suitable states of the endogenous electromagnetic fields in a living system observed as biophotons. These states give rise to sub, super, and simply Poisson photo count distributions at different levels of squeezing and displacement. This was the main motivation for investigating the possibility of representing a biophoton signal by a squeezed state.

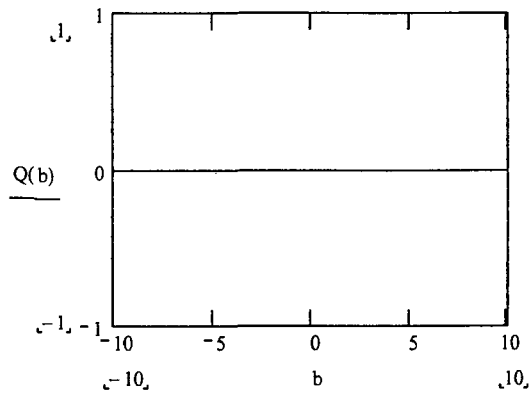


Fig: 5(a)

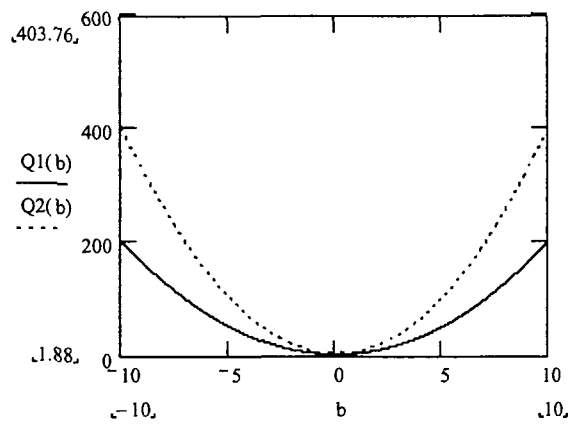


Fig: 5(b)

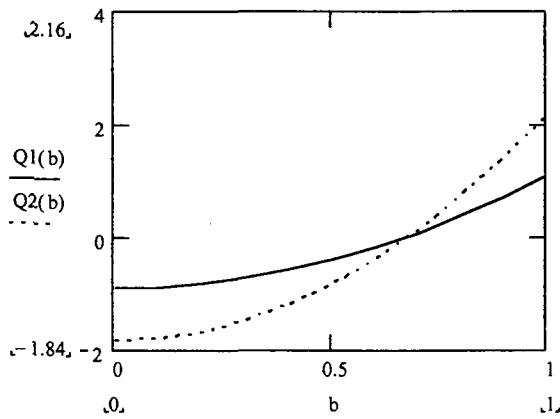


Fig: 5(c)

Fig: 5. Q-value versus  $\text{Im}(\alpha)$  in excited number states; (a).  $\text{Re}(\alpha) = 1.2$  and  $n = 0$   
 (b).  $\text{Re}(\alpha) = 1.2$  and  $n = 1, 2$ ; (c).  $\text{Re}(\alpha) = .2$  and  $n = 1, 2$ .

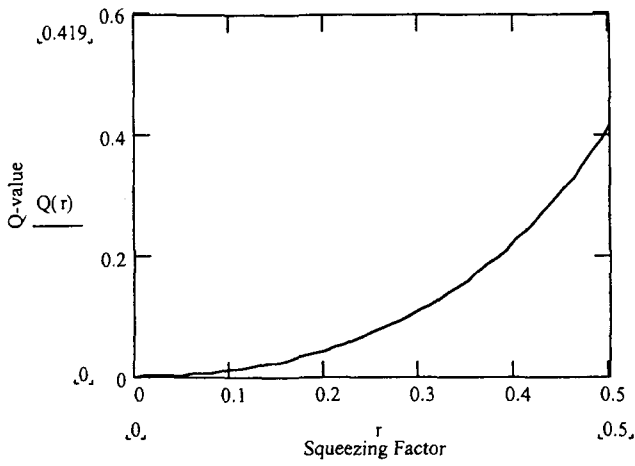


Fig: 6(a)

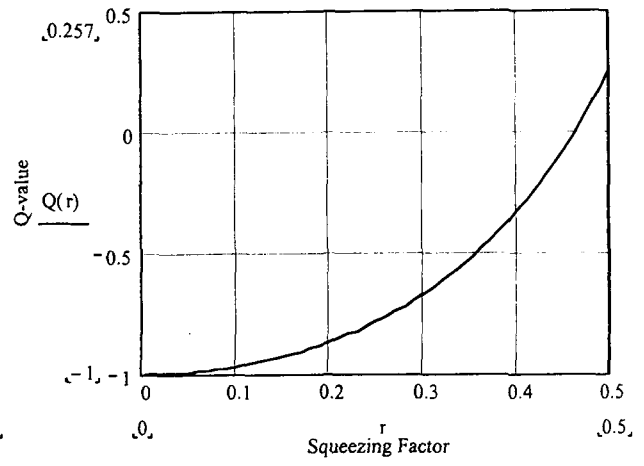


Fig: 6(b)

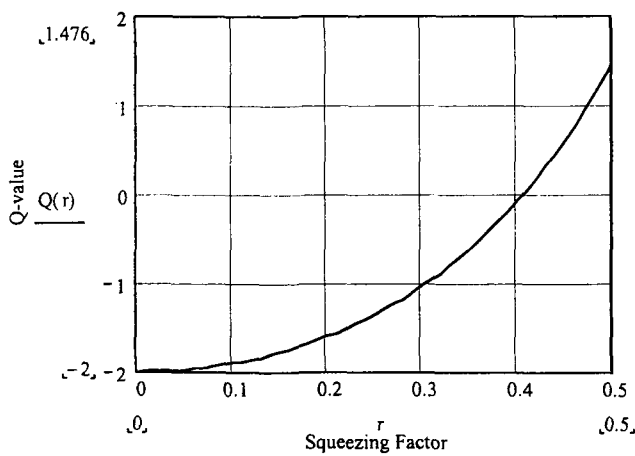


Fig: 6(c)

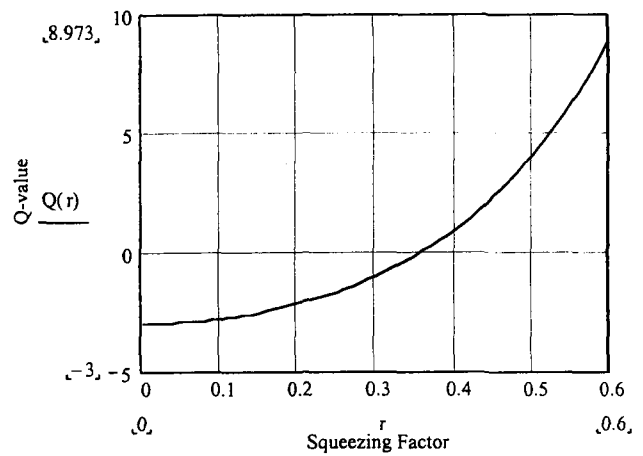


Fig: 6(d)

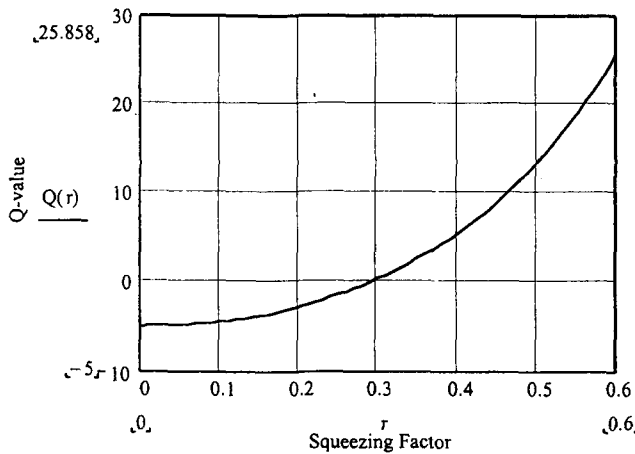


Fig: 6(e)

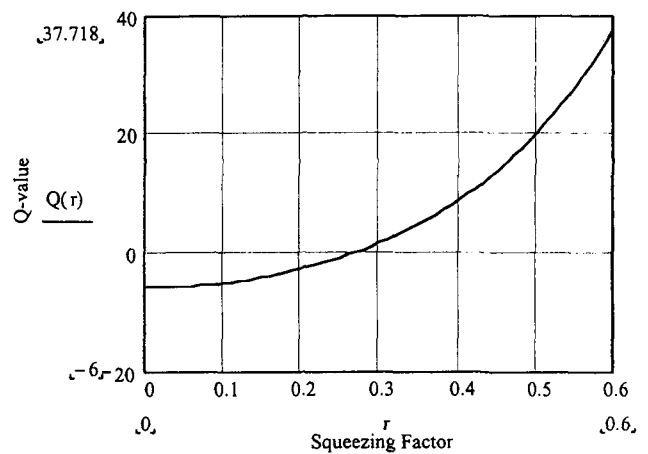


Fig: 6(f)

Fig: 6. Q-value versus Squeezing factor in Squeezed Number States with  $n = 0, 1, 2, 3, 5$  and  $6$  in 6(a), 6(b), 6(c), 6(d), 6(f) and 6(e) respectively.

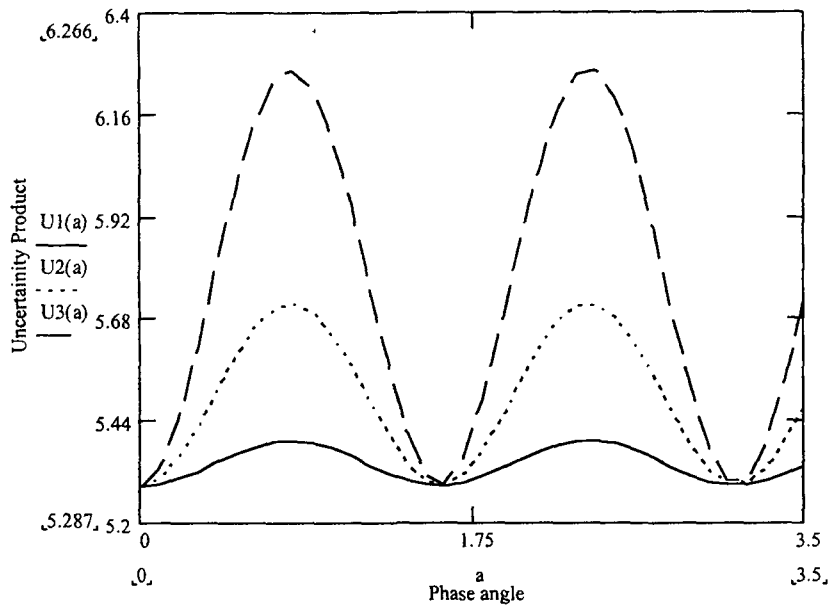


Fig: 7(a)

Fig: 7(a). Uncertainty Product versus Phase angle in Squeezed number states;  $n=0$   
 $r = .1, .2, .3$ .

7(b). Uncertainty Product versus Phase angle in Squeezed number states;  $r = .4$   
 $n = 0, 1$  and  $2$ .

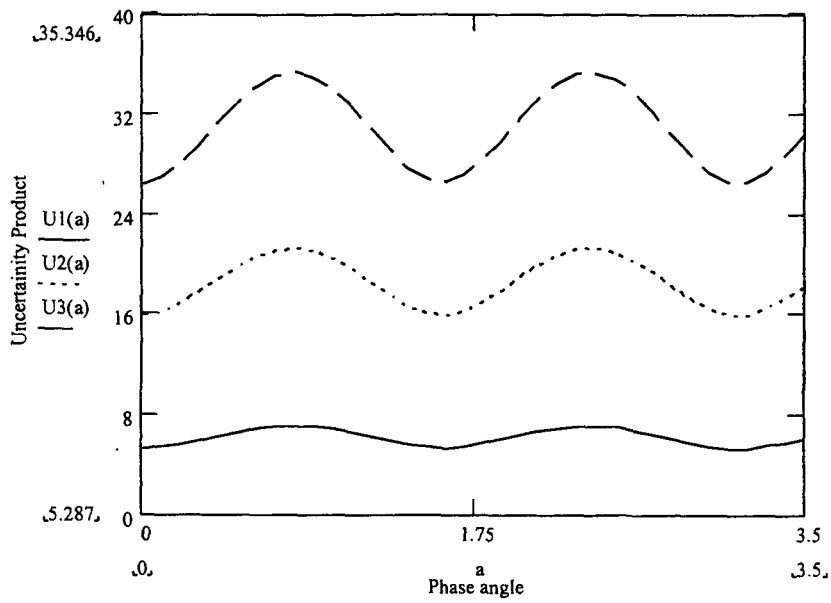


Fig: 7(b)

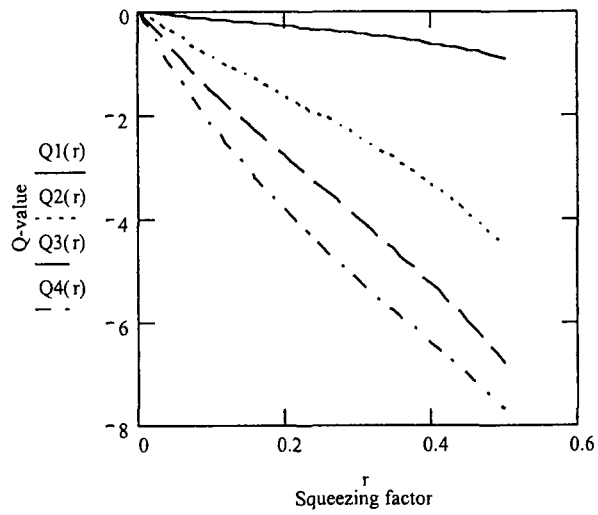


Fig: 8(a)

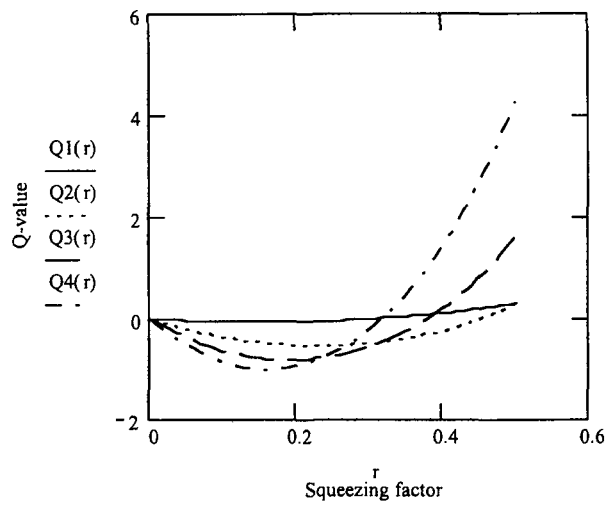


Fig: 8(b)

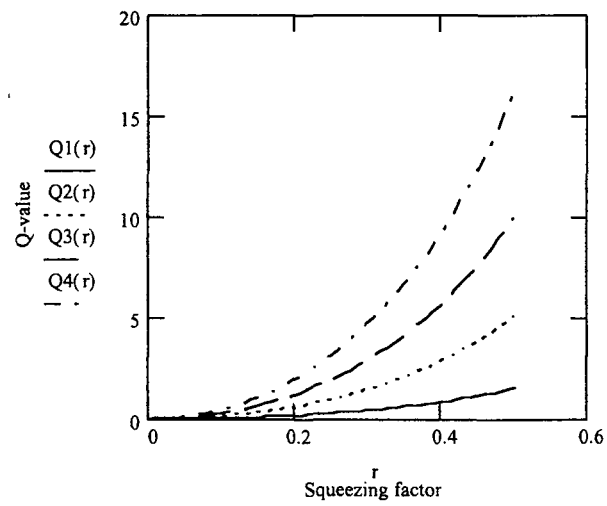


Fig: 8(c)

Fig: 8. Q-value v/s Squeezing factor in  $|\varepsilon, \alpha, n\rangle$  states for  $|\alpha|^2 = .5$  and  $n = 0, 1, 2$  and  $3$   
 (a), (b) and (c) are for phase angles  $\phi = 0, 30$  and  $45$

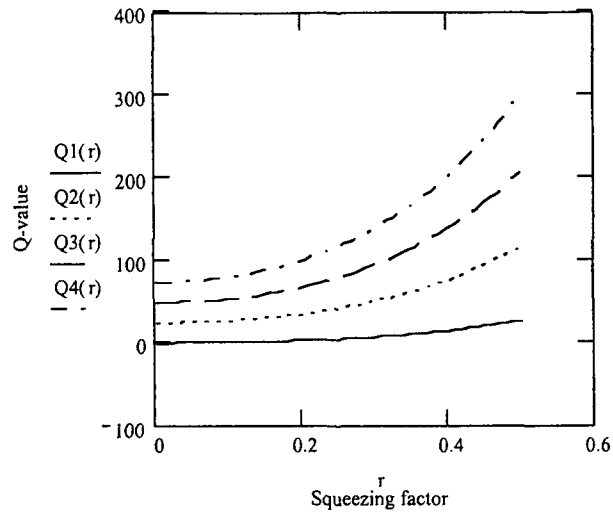


Fig: 9(a)

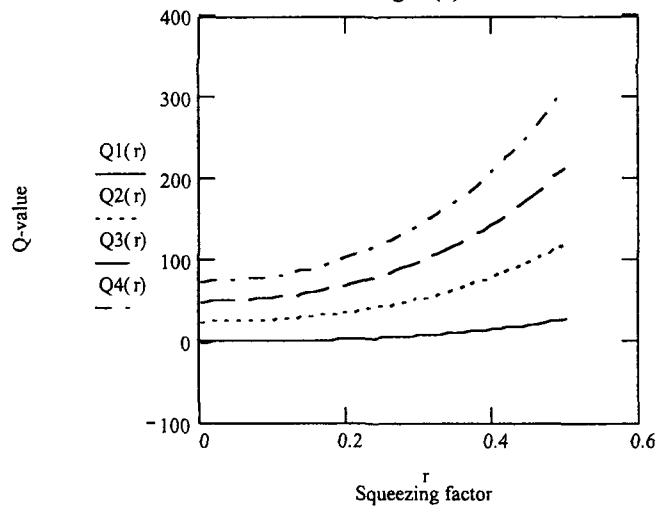


Fig: 9(b)

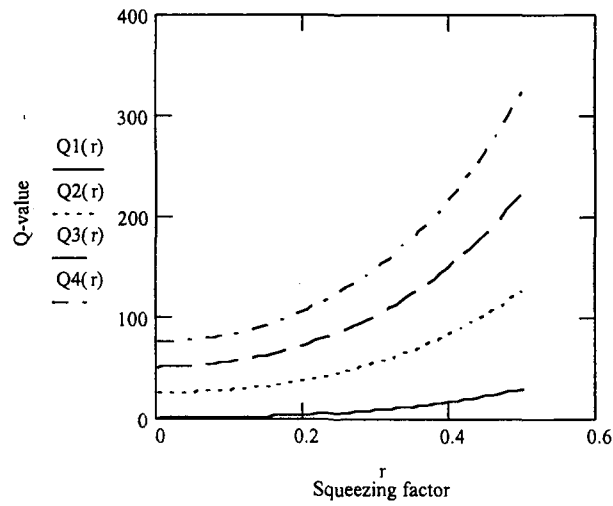


Fig: 9(c)

Fig: 9. Q-value versus Squeezing Factor in  $|\varepsilon, \alpha, n\rangle$  states for  $|\alpha|^2 = 13$   
 $n = 0, 1, 2$  and  $3$ ; (a), (b) and (c) are for Phase angles  $\phi = 0, 30$  and  $45$ .

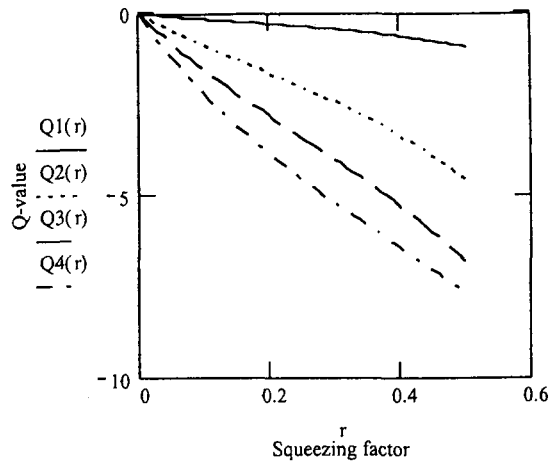


Fig: 10(a)

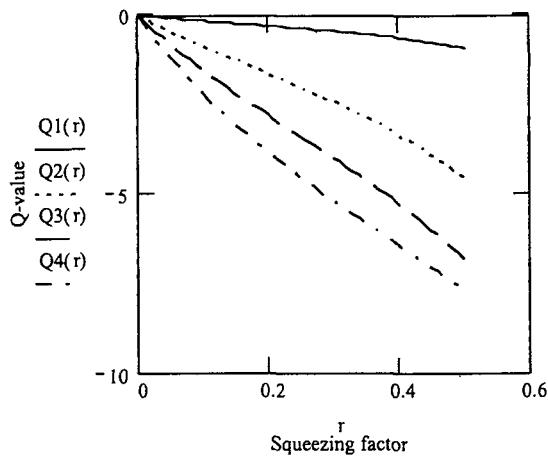


Fig: 10(b)

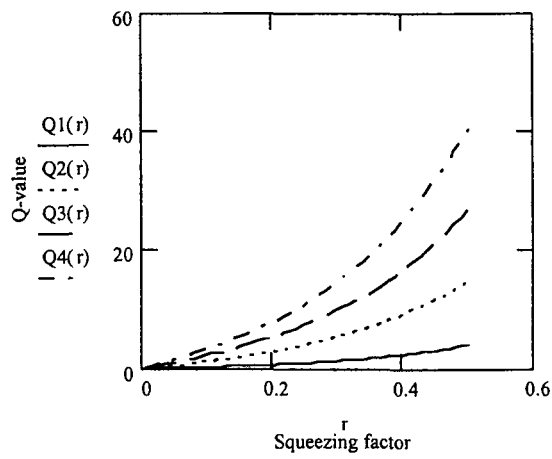


Fig: 10(c)

Fig: 10. Q-value v/s Squeezing factor in  $|\varepsilon, \alpha, n\rangle$  states for  $n = 0, 1, 2$  and  $3$   
 $|\alpha|^2 = .5$ ; (a), (b) and (c) are for phase angles  $0, 180$  and  $90$  respectively.

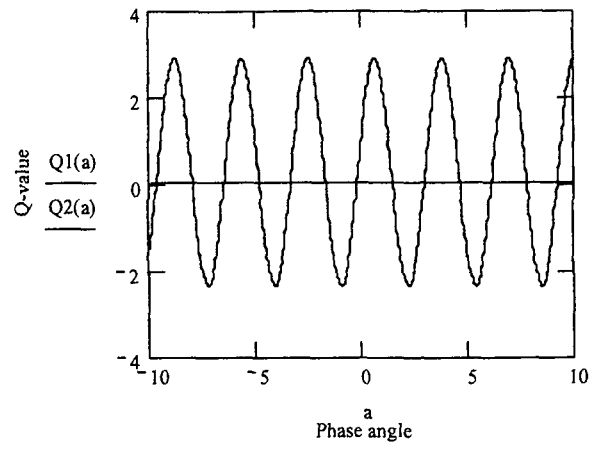


Fig: 11(a)

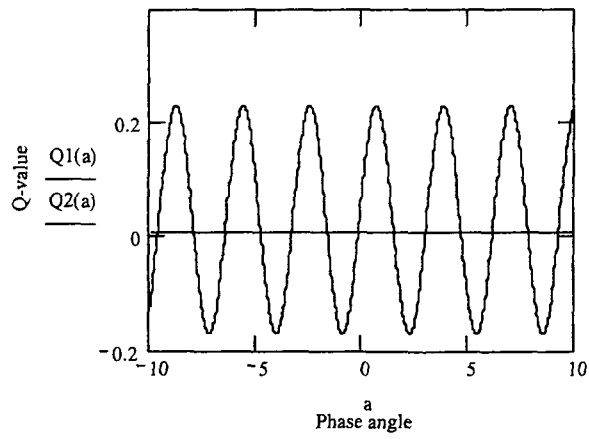


Fig: 11(b)

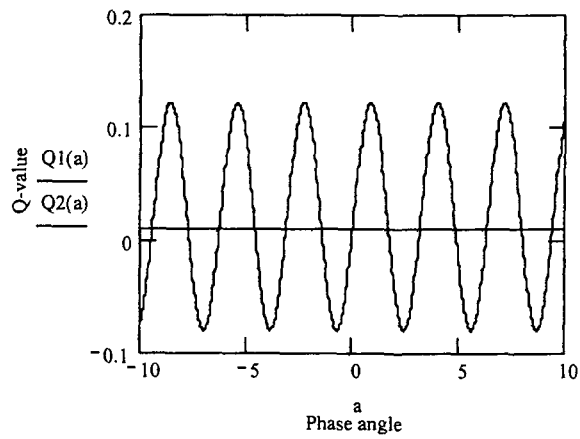


Fig: 11(c)

Fig: 11. Q-values v/s Phase angle in  $|\alpha, \varepsilon, n\rangle$  states for  $n = 0; r = .1$

(a).  $|\alpha|^2 = \frac{1}{2}$ ; (b).  $|\alpha|^2 = 1$ ; (c).  $|\alpha|^2 = 5$ .

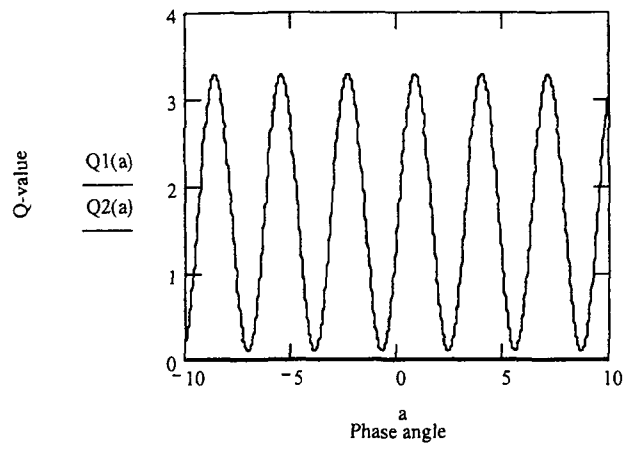


Fig: 12(a)

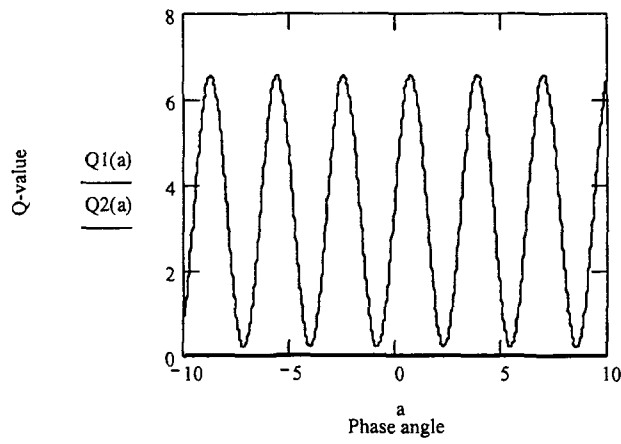


Fig: 12(b)

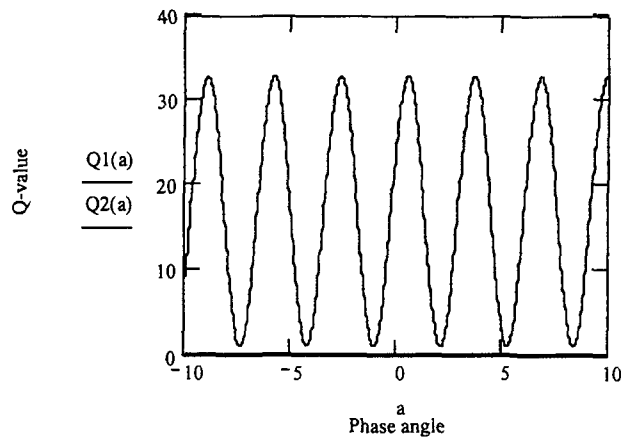


Fig: 12(c)

Fig: 11. Q-value v/s phase angle in  $|\alpha, \varepsilon, n\rangle$  states for  $n = 1; r = .1; (a). |\alpha|^2 = .5;$

(b).  $|\alpha|^2 = 1; |\alpha|^2 = 5$

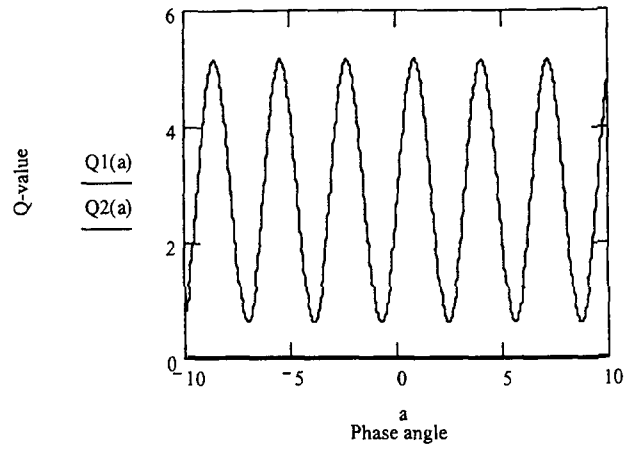


Fig: 13(a)

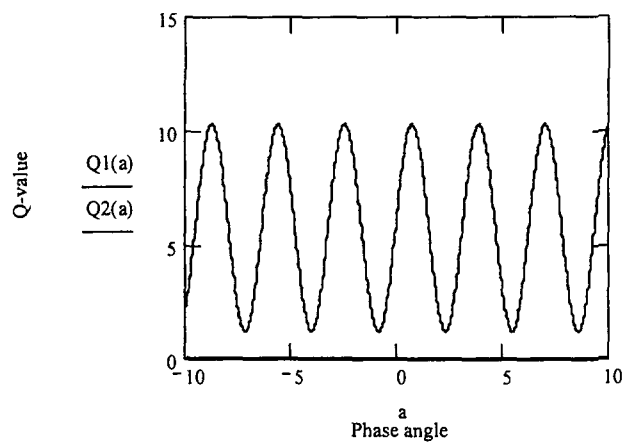


Fig: 13(b)

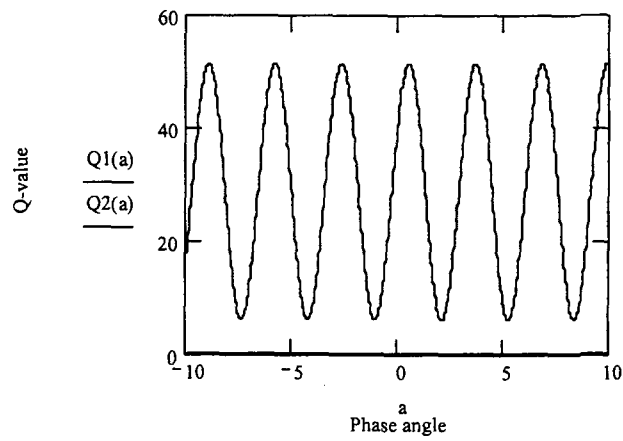


Fig: 13(c)

Fig: 13. Q-value v/s phase angle in  $|\alpha, \varepsilon, n\rangle$  states for  $n = 2$  and  $r = .407$ ; (a).  $|\alpha|^2 = .5$   
 (b).  $|\alpha|^2 = 1$ ; (c).  $|\alpha|^2 = 5$ .

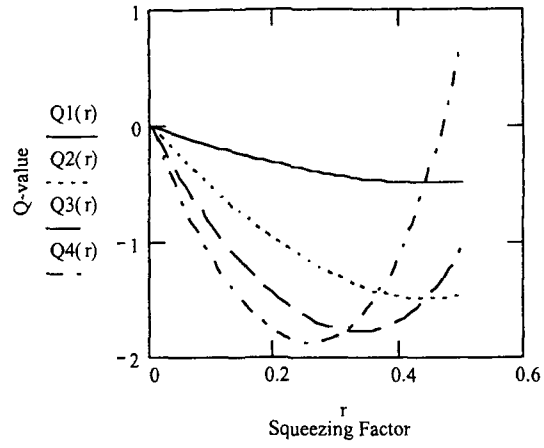


Fig: 14(a)

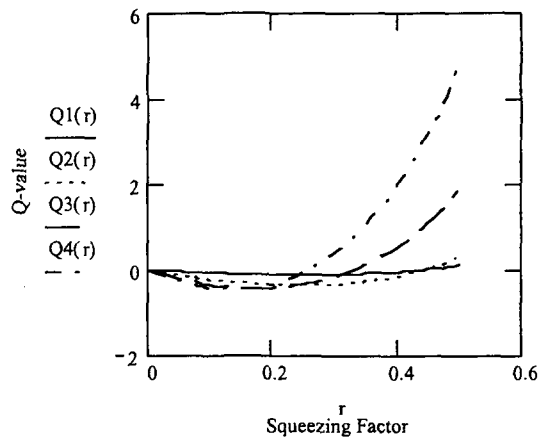


Fig: 14(b)

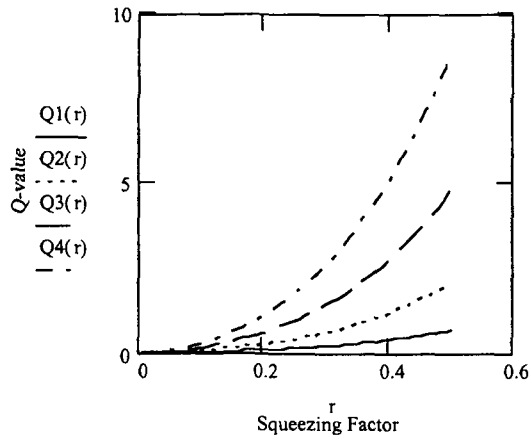


Fig: 14(c)

Fig: 14. Q-value v/s squeezing Factor in  $|\alpha, \varepsilon, n\rangle$  states for  $|\alpha|^2 = .5$ ;  $n = 0, 1, 2$  and  $3$  (a), (b) and (c) for phase angles  $0, 30$  and  $45$  respectively.

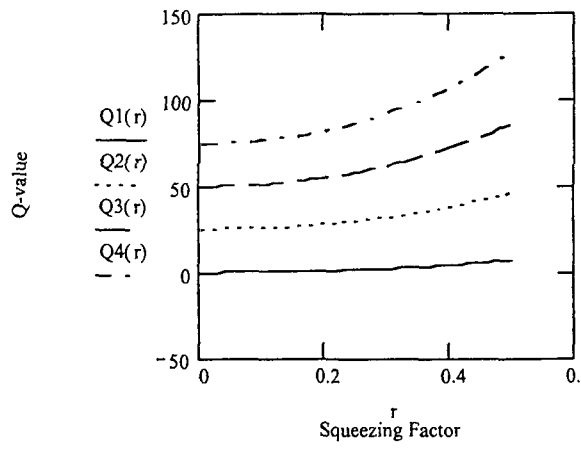


Fig: 15(a)

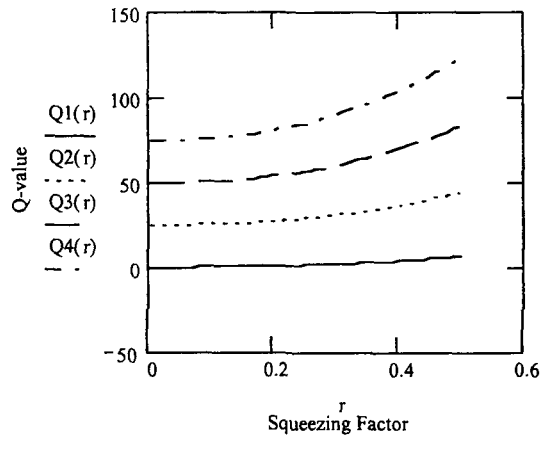


Fig: 15(b)

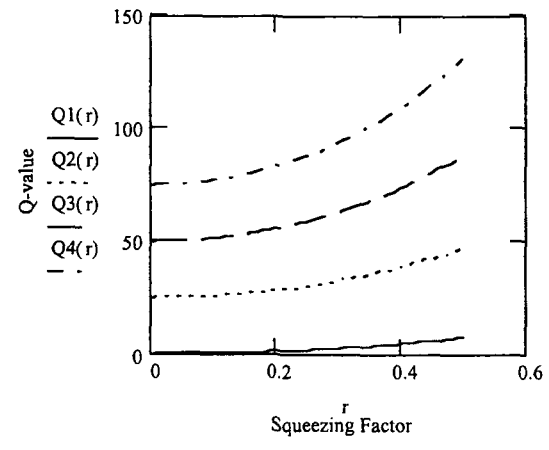


Fig: 15(c)

Fig: 15. Q-values v/s Squeezing factor in  $|\alpha, \varepsilon, n\rangle$  states for  $|\alpha|^2 = 13$   
 $n = 0, 1, 2$  and  $3$ ; (a), (b) and (c) are for phase angle  $= 0, 30, 45$  respectively.

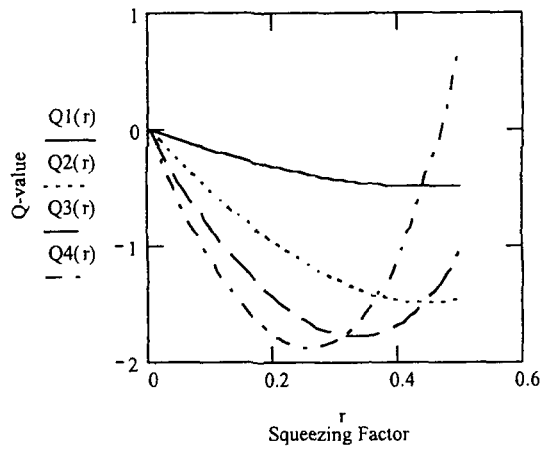


Fig: 16(a)

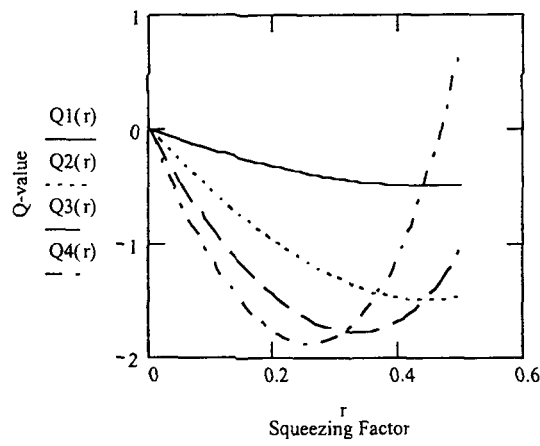


Fig: 16(b)

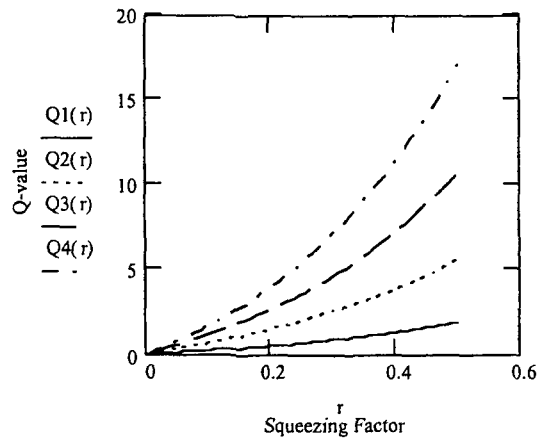


Fig: 16(c)

Fig: 16. Q-value v/s Squeezing factor in  $|\alpha, \varepsilon, n\rangle$  states for  $n = 0, 1, 2$  and  $3$ ;  $|\alpha|^2 = .5$   
(a), (b) and (c) for phase angle  $0, 180, 90$  respectively.

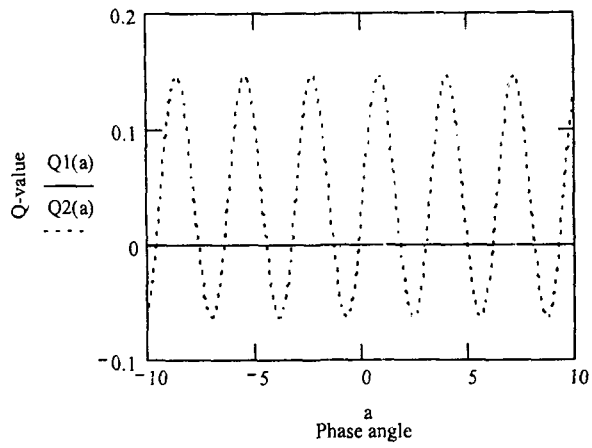


Fig: 17(a)

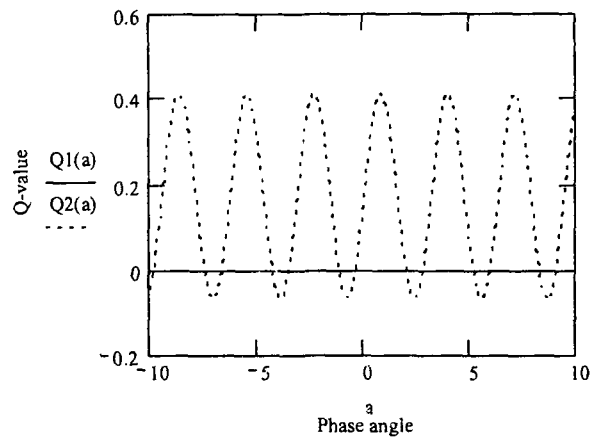


Fig: 17(b)

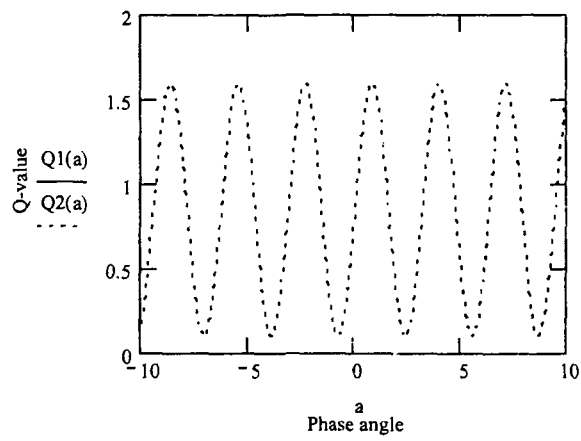


Fig: 17(c)

Fig: 17. Q-value v/s Phase angle in  $|\varepsilon, \alpha\rangle$  state for  $|\alpha|^2 = .5$ ; (a).  $r = .1$ ;  $r = .2$ ;  $r = .4$ .  
The line in the back ground corresponds to displaced vacuum.

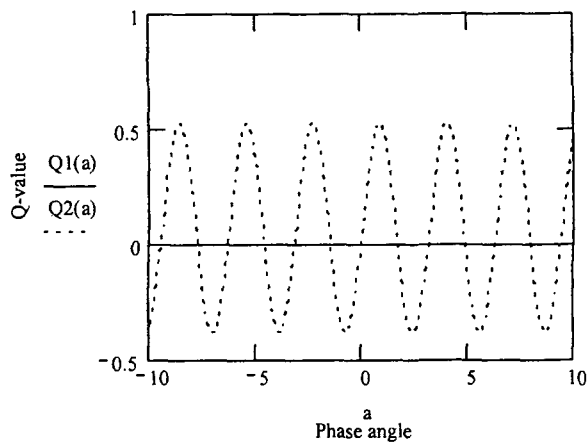


Fig: 18(a)

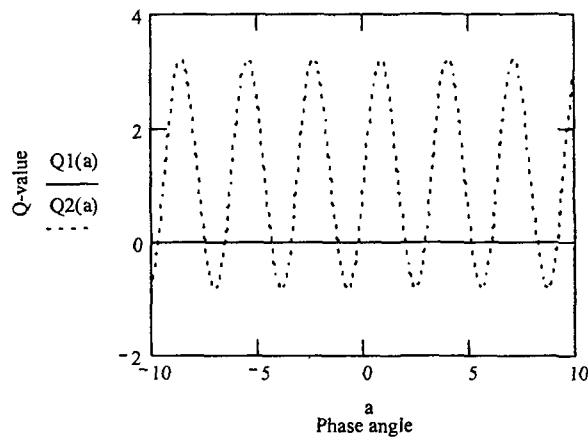


Fig: 18(b)

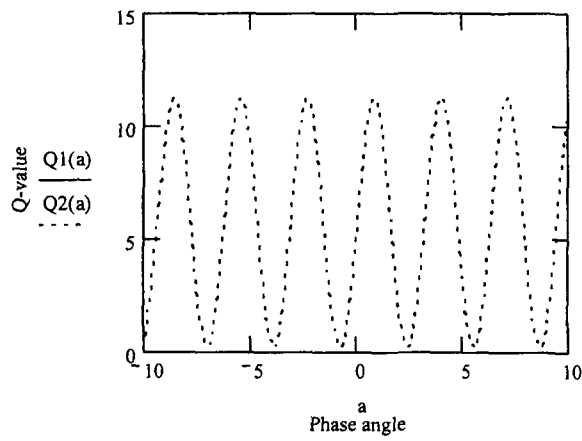


Fig: 18(c)

Fig: 18. Q-value v/s phase angle in  $|\varepsilon, \alpha, n\rangle$  states for  $|\alpha|^2 = .5$ ;  $n = 2$ ; (a).  $r = .05$   
 (b).  $r = .2$ ; (c).  $r = .4$ .

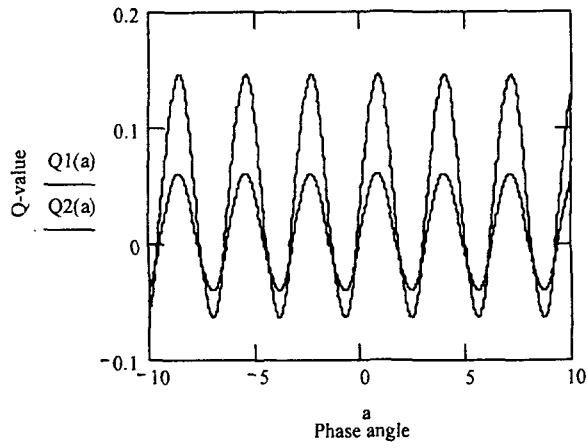


Fig: 19(a)

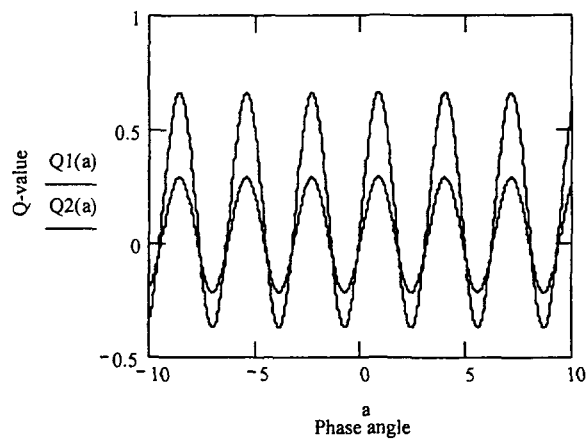


Fig: 19(b)

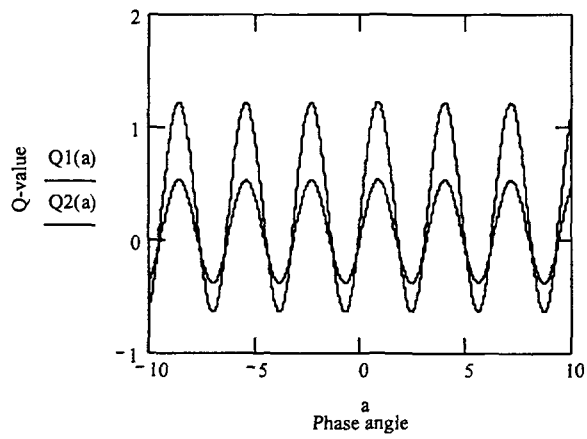


Fig: 19(c)

Fig: 19. Q-values v/s phase angle in  $|\varepsilon, \alpha, n\rangle$  states for  $|\alpha|^2 = .5$ ;  $r = .05, .1$   
 (a).  $n = 0$ ; (b).  $n = 1$ ; (c).  $n = 2$ .

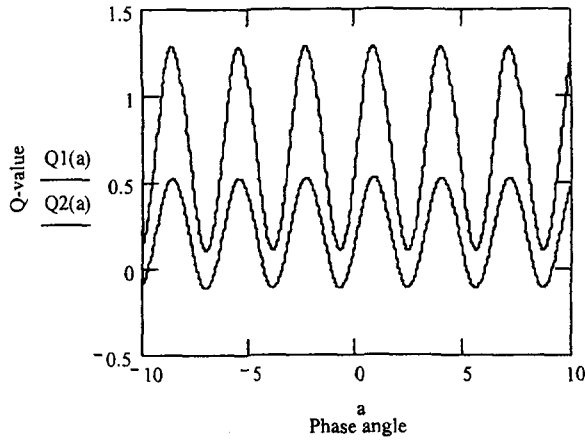


Fig:20(a)

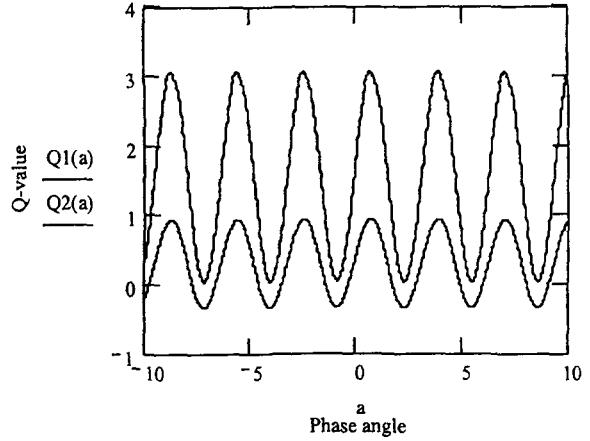


Fig:20(b)

Fig: 20(a). Q-value v/s Phase angle in  $|\alpha, \varepsilon\rangle$  states for  $|\alpha|^2 = .5$ ;  $r = .3, .5$ .

Fig: 20(b). Q-value v/s Phase angle in  $|\alpha, \varepsilon\rangle$  states for  $|\alpha|^2 = 1$ ;  $r = .3, .6$ .

Fig: 20(c). Q-value v/s Phase angle in  $|\alpha, \varepsilon\rangle$  states for  $|\alpha|^2 = 5$ ;  $r = .3, 1$ .

Fig: 20(d). Q-value v/s Phase angle in  $|\alpha, \varepsilon\rangle$  states for  $|\alpha|^2 = 10$ ;  $r = .3, 1.2$ .

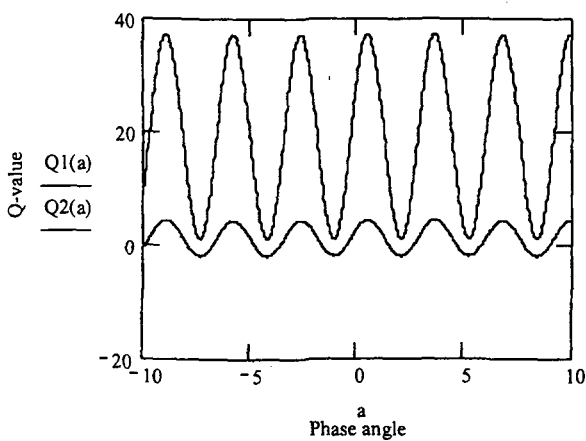


Fig:20(c)

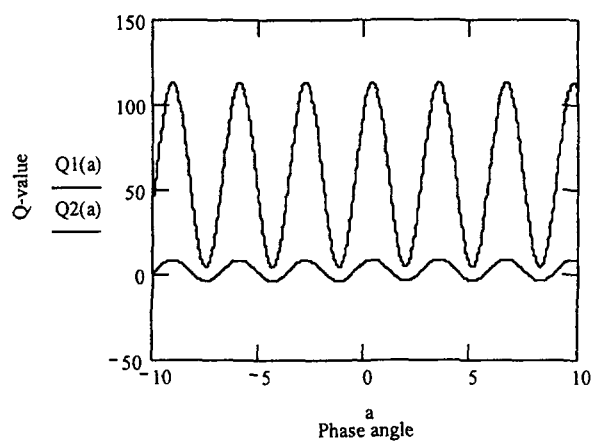


Fig:20(d)

## Chapter 4

### A Phenomenological Model of Biophoton Emission

**4.1 Introduction:** The study of the properties of the squeezed state of photon prepares us to suggest a phenomenological model for describing biophoton signals. Let us recapitulate the important unexplained properties of biophoton signals. Biophoton emission is the emission of photons of ultra weak intensity by a biological system, which can be any living system from bacteria to human tissues <sup>[20]</sup>. A Biophoton signal depends upon many environmental and physiological factors, like temperature, humidity and health. The signal appears to be situation and system specific. The specificity is manifested through the dependence of the shape of the signal various factors. The specificity rules out the origin of biophotons from chemiluminescence, bioluminescence, fluorescence and super fluorescence <sup>[20-22]</sup>. The origin and source of biophotons <sup>[23]</sup> has not been established so far. Biophoton emission has been assumed to be of two different kinds - spontaneous and stimulated emissions <sup>[21,25]</sup> – because of its history. The photon flux in spontaneous emission is ultra weak and remains nearly unchanging for hours. Its measurement requires sensitive detectors approaching the quantum mechanical limit. The photon flux in light induced emission is more intense but lasts only for a short while <sup>[24]</sup>. The signal is observed to decay to the level of spontaneous emission within few minutes. The decay shows non-exponential relaxation behaviour <sup>[25]</sup>. The strength of the signal varies from system to system. The light

induced emission is found to be more intense in photosynthetic systems. The peak intensity of the signal is two three orders of magnitude higher than intensity of the signal <sup>[26]</sup> in spontaneous emission

The experimental data have been parametrized using multi- exponential functions <sup>[27,28]</sup>, hyperbolic <sup>[29]</sup> and other type of functions <sup>[30]</sup>. Constant flux in spontaneous emission and non-exponential relaxation behaviour in the light induced emission are two prominent and unexplained characteristics. It is difficult to incorporate them in any semi classical model. One requires a new approach to understand biophoton emission. We suggest dividing the problem of biophoton emission into parts- origin of a biophoton signal, its description and the purpose of its emission. The origin and purpose of biophoton signals belong to philosophical and speculative considerations. The description of the signal is a valid scientific problem and various attempts made in solving the problem are influenced by philosophical considerations. Alexander Gurvich <sup>[4]</sup> pioneered two ideas on its origin and hypothesized that biophotons originate from free radical reactions, and biophoton emission comes from an organized morphogenetic field that is at the basis of life. Gurvich did not considered these hypotheses to be contradictory. A contradiction arose because of the subsequent scientific developments. The origin of biophotons from free radical reactions belongs to the reductionist biochemical approach. The

biophotons in this approach can arise from random metabolic imperfections and should show exponential decay and Gaussian distribution. The association of biophotons with some organized morphogenetic field requires the discovery of a morphogenetic field and coherency in the biophoton signal. The coherency of a biophoton signal has to be investigated by following a quantum optical approach. The quantum approach is more appropriate for single determined from single photo count measurements. Our investigations presented in the previous two chapters give the necessary background material for the quantum approach.

#### **4.2. Biophoton Emission from a Coherent Light Field:**

Coherence theory based on the physics of interactions of weak radiation in and with optically dense matter, claims that biophoton emission originates from a delocalized coherent electromagnetic field within the living tissue, in particular from its optical modes <sup>[25]</sup>. Coherence theory is based on the formation of networks of exciplexes like coherent excitations in living matter. It explains the low intensity biophoton signal in terms of fairly high degree of coherence of non-classical light with very high signal to noise ratio. Experimental data on biophotons are in complete agreement with the hypothesis that a coherent field is the source of biophoton emission <sup>[25]</sup>.

Photo count distribution of biophotons emitted in the quasi-stationary states is generally Poissonian. A multimode chaotic field with coherent time,  $\tau$  much smaller than the measurement time interval  $\Delta t$ , the geometrical distribution approaches Poissonian. Hence a Poissonian photo count statistics alone cannot indicate the presence of coherent field. Evidence of coherence comes from

1. Non-linear optical transparency of biophotons through matter [31].
2. Hyperbolic relaxation kinetics under ergodic conditions after illumination [32].
3. Observed sub Poissonian photo count statistics displays a collective excitation with high degree of coherence.
4. Biological systems also tend to display a super Poissonian distribution also, which is believed to be due to rhythms of biophoton emission [25].

Classical description of coherence is not sufficient for understanding the coherence in weak light emission. Since only single quantum is counted the phenomenon is subjected to real quantum effect. A fully coherent field in a stationary state is always subjected to Poissonian photo count distribution and under ergodic conditions a hyperbolic decay is a sufficient condition of coherent field. Hyperbolic decay of a single mode after

exposure to light has been demonstrated which indicates a fully coherent field <sup>[32]</sup>. It was shown that coherent field remains coherent during time evolution according to Hyperbolic rather than an exponential law. Relaxing ergodic systems, either shows an exponential decay of the form  $n \propto e^{-\lambda t}$  or a hyperbolic decay of the form  $n \propto \frac{1}{t}$ . Where n is the number of radiating atoms or molecules  $\lambda$  is the decay constant and t is the time. The quantum description of exponential decay <sup>[33]</sup> and hyperbolic decay <sup>[32]</sup> has been cited.

Hyperbolic decay has been shown as a signature of fully coherent field that always displays Poissonian distribution at any instant <sup>[32]</sup>. Hyperbolic relaxation seems to be common in biological systems e.g., white light induced reemission of photons from cell <sup>[34]</sup>. It was regarded as a powerful tool for analyzing the living state in terms of its coherence <sup>[36]</sup>.

#### **4.3 Description of Biophoton Field by a Damped Harmonic**

**Oscillator:** The study of harmonic oscillator with time dependent mass and frequency is of profound value for understanding the problems of radiation from biological systems. Jannussis et.al. <sup>[36]</sup> has shown that excited states of such a harmonic oscillator are equivalent to squeezed states. A damped harmonic oscillator, if it interacts with its surrounding radiation field in a coherent way, may not follow the exponential time dependence of the damping terms. Li <sup>[37]</sup>, therefore, replaced the

constant damping term by a function of time  $2\lambda(t)$  and determined its functional form by the requirement of frequency stability. Li argued that the phenomenological damping term somehow represent the effect of a mechanism that invokes a cooperative behaviour among several molecules in living systems. He further suggested that biophotons are emitted in some non-classical state of electromagnetic field. The nature of decay depends on the manner in which system interacts with the living system. In the absence of explicit knowledge about this interaction representation of the time evolution of the field by a damped harmonic oscillator with time dependent mass and frequency may be justified.

There is a need to construct a definite model for exploring the potentialities inherent in the speculations of Popp and Li. We, therefore, assume that an endogenous electromagnetic field in pure quantum state is associated with all living system and the quantum state of the field is a squeezed state of photon generated by a frequency stable damped harmonic oscillator. Our assumption is essential for concretizing the speculations of Popp and Li. The assumption allows us to make definite prediction for measurable quantities. The assumption may appear preposterous and is difficult to justify on the basis scientific knowledge of non-living matter. The most objectionable feature of the assumption is its implication that quantum coherence of the biophoton field is sustained during the entire life of a living system. We are

unable to provide a satisfactory rebuttal to this objection. We can only say that a living system does exhibit coherence in its entire life and the emergence of its coherence from some quantum effects is not ruled out. Biophoton field is a reminiscence of the unknown quantum processes occurring in living systems. The study of the biophoton signals may throw some light on these processes. The presence of quantum electromagnetic field in a living system is desirable for explaining many properties. Such a field can obviate the need of morphogenetic fields and may be able to explain the long-range spatio-temporal coherence and co-operative behaviour of biomolecules in living systems<sup>[25]</sup>. If the quantum state of this field happens to be a squeezed state then it is possible to adjust the degree of coherence and the extent of delocalization of the field by varying the uncertainty in either of the two canonically conjugate variables<sup>[38]</sup> over a wide range of values. The possibility that the uncertainty in one variable can be made very small in a squeezed state makes squeezed states more suitable for signal communication and information transfer. Let us, therefore, accept the assumption and investigate its various verifiable consequences.

The solution of the problem of damped harmonic oscillator requires specification of boundary conditions, which will also determine the specific quantum state of the field in the quantum context. The damped harmonic oscillator will govern the evolution of field. The field will show an explicit dependence in addition to the harmonic variation

arising from mode frequency. The explicit time dependence will determine the broad characteristics of the signal. The finer characteristics of the signal will be determined by the quantum state. These finer characteristics are influenced by the boundary conditions that are essential in specifying the quantum state of the field. The influence of the boundary conditions makes a biophoton signal situation specific. Many exogenous and endogenous factors determine the boundary conditions. External light is an exogenous factor that stimulates most living systems by altering the state of their associated biophoton field. The quantum evolution of the altered field is different from the one, which has existed before, and hence the stimulated system may show a change in pattern of photon emission. This is a qualitative explanation of the phenomenon of light induced biophoton emission. We can make it quantitative by calculating the time dependence of various measurable quantities in the state of associated biophoton field. In particular, the expectation value of the photon number operator gives the intensity of the field <sup>[39]</sup> and its time dependence or relaxation behaviour gives the shape of the signal. We explicitly calculate it in the next section. The calculation shows that the leading contribution to the intensity has two terms. One term is time independent and the other has non-exponential decaying time dependence. The time independent term is responsible for spontaneous biophoton emission; whereas the time dependent term represents the

relaxation behaviour. The relative strength of the two terms depends upon the boundary conditions. It, therefore, varies from system to system and shows dependence upon physiological and environmental factors. We have also calculated the uncertainty product of position and momentum operators. The calculations point out the closeness of the state of the biophoton field to a minimum uncertainty state. We have also determined the variance of photon number in order to learn the nature of photo count statistics.

#### 4.4 Mathematical formulation of the model

A single mode free electromagnetic field of frequency  $\omega$  is described by the harmonic oscillator Hamiltonian

$$H_0 = \frac{1}{2}\omega^2 x^2 + \frac{1}{2}P_x^2 \quad (1)$$

Where  $x$  and  $P_x$  are canonically conjugate position and momentum variables related to electric and magnetic field components. The equation of motion for a simple harmonic oscillator is

$$\frac{d^2x}{dt^2} + \omega^2 x = 0. \quad (2)$$

Quantisation of the system gives the usual creation operator  $a^+$  and annihilation operator  $a$ , of the photon. All measurable quantities are expressed with these operators, e.g. photon number by the operator  $a^+a$ . Number states, coherent states and squeezed states (also called two

photon coherent states) are eigen states of the operator  $\mathbf{a}^+ \mathbf{a}$ ,  $\mathbf{a}$  and  $\mathbf{b}$  respectively. The operator  $\mathbf{b}$  is related to operator  $\mathbf{a}$  and  $\mathbf{a}^+$  by <sup>[19]</sup>.

$$\mathbf{b} = \mu \mathbf{a} + \nu \mathbf{a}^+ \quad (3)$$

Where  $\mu$  and  $\nu$  are arbitrary parameters satisfying the constraint

$$|\mu|^2 - |\nu|^2 = 1 \quad (4)$$

All pairs  $(\mu, \nu)$  introduced subsequently will satisfy the above equation. The transformation from  $(\mathbf{a}^+, \mathbf{a})$  to  $(\mathbf{b}^+, \mathbf{b})$  is a unitary transformation and preserves the commutation relation  $[\mathbf{a}, \mathbf{a}^+] = [\mathbf{b}, \mathbf{b}^+] = 1$ . Consequently, the pair  $(\mathbf{b}^+, \mathbf{b})$  give another particle description, these particles are called quasi particles. A quasi particle is annihilated by operator  $\mathbf{b}$  and created by operator  $\mathbf{b}^+$ . By inverting (3) we get

$$\mathbf{a} = \mu^* \mathbf{b} - \nu \mathbf{b}^+ \quad (5)$$

A squeezed state of the photon will be represented by  $|\beta, \mu, \nu\rangle$ . It is an eigen state of the quasi particle operator with complex eigen value  $\beta$ . The expectation values of the measurable quantities in the squeezed state can be calculated with the help of (5). We give below the values of photon number  $\langle n \rangle$ , uncertainty product  $\Delta x \Delta p$  and  $Q = \langle \Delta n^2 \rangle - \langle n \rangle$  as <sup>[39,40]</sup>.

$$\langle n \rangle = |\nu|^2 + |\mu^* \beta - \nu \beta^*|^2 \quad (6)$$

$$\Delta x \Delta p_x = \frac{\hbar}{2} \sqrt{|\mu + \nu| |\mu - \nu|} \quad (7)$$

And

$$Q = 2|\nu|^4 + |\nu|^2 + 2|\beta|^2(4|\nu|^2 + 3)|\nu|^2 - 2\text{Re}(\beta^* \mu \nu)(4|\nu|^2 + 1) \quad (8)$$

Pedrosa <sup>[41]</sup> has shown that coherent states of an oscillator with time dependent damping and mass terms are equivalent to the squeezed state of the free oscillator. The dynamics of a time dependent harmonic oscillator is governed by the following equation <sup>[36]</sup>.

$$\frac{d^2 q}{dt^2} + 2\lambda(t) \frac{dq}{dt} + \omega^2(t)q = 0 \quad (9)$$

Where  $q$  is a position variable,  $\lambda(t)$  a time dependent damping coefficient and  $\omega(t)$  is a time dependent frequency term. The system has a quasi particle interpretation in Quantisation. It is similar to the free field description in which photons are replaced by quasi particles. The quasi particle operators  $\mathbf{b}(t)$  and  $\mathbf{b}^\dagger(t)$  are determined <sup>[36]</sup> by the solution of (9). It also determines the evolution of a state. It is such that an eigen state of the time dependent operator  $\mathbf{b}(t)$  continues to remain in its eigen state with the same eigen value <sup>[36]</sup>. It resembles the evolution in an undamped oscillator, where a coherent state remains a coherent state with the same eigen value during evolution <sup>[39]</sup>. Operators  $\mathbf{b}(t)$  and  $\mathbf{b}^\dagger(t)$  are related to the photon operators by a linear unitary transformation. As a result, a coherent state of the quasi

particle is also a squeezed state of the photon. A squeezed state of the photon evolves into another squeezed state in the dynamics given by (9).

Damping usually alters the mode frequency. If damping is time dependent, then the frequency also varies with time. Variable frequency is not desirable if one hopes to assign a role to biophotons <sup>[20,21]</sup> in signal communication and in maintaining the biological integrity of the system. One, therefore, imposes the requirement of frequency stability. It is achieved by taking <sup>[42]</sup>

$$\lambda(t) = \frac{\lambda_0}{1 + \lambda_0 t} \quad (10)$$

Where  $\lambda_0$  is an arbitrary real constant. It gives the damping coefficient at  $t=0$ . The Hamiltonian of the system for any stable frequency  $\omega$  now becomes

$$H = \frac{\mathbf{p}^2}{2(1 + \lambda_0 t)^2} + \frac{1}{2}(1 + \lambda_0 t)^2 \omega^2 \mathbf{q}^2 \quad (11)$$

The solution of (9) for the above damping easily obtained. Following Jannussis and Bartzis <sup>[36]</sup> we express the quasi particle operator  $\mathbf{b}(t)$  in terms of the quasi particle operators at  $t = 0$ . It gives

$$\mathbf{b}(t) = \mu(t)\mathbf{b}(0) + \nu(t)\mathbf{b}^+(0) \quad (12)$$

With

$$\begin{aligned}\mu(t) &= \cos\omega t + \frac{\lambda_0}{2\omega} \frac{\lambda_0 t}{2\omega(1+\lambda_0 t)} \sin\omega t \\ &+ i \frac{\lambda_0}{2\omega} \frac{\lambda_0 t}{(1+\lambda_0 t)} \cos\omega t - i \left\{ 1 + \frac{\lambda_0^2}{2\omega^2(1+\lambda_0 t)} \right\} \sin\omega t\end{aligned}\quad (13)$$

And

$$\begin{aligned}\nu(t) &= \frac{\lambda_0}{2\omega} \left\{ 1 + \frac{1}{(1+\lambda_0 t)} \right\} \sin\omega t \\ &+ i \frac{\lambda_0}{2\omega} \frac{\lambda_0 t}{(1+\lambda_0 t)} \cos\omega t - i \frac{\lambda_0^2}{2\omega^2(1+\lambda_0 t)} \sin\omega t\end{aligned}\quad (14)$$

The state of the field at  $t = 0$  is an eigen state of a quasi particle operator  $\mathbf{b}(t)$  and contains information about the living system and its environment. If the field at  $t = 0$  is taken to be in a state  $|\beta, \mu_0, \nu_0\rangle$  with  $\beta, \mu_0$  and  $\nu_0$  as input parameters, then

$$\mathbf{b}(0) = \mu_0 \mathbf{a} + \nu_0 \mathbf{a}^+ \quad (15)$$

The state  $|\beta, \mu_0, \nu_0\rangle$  will evolve<sup>[39]</sup> into another state  $|\beta, \mu_t, \nu_t\rangle e^{i\phi}$ .

Since the phase  $\phi(t)$  of the state does not enter our calculations it need not be determined. We can determine the parameters  $\mu_t$  and  $\nu_t$  by noting that the quasi particle operator  $\mathbf{b}(t)$  of the evolved state is given by

$$\mathbf{b}(t) = \mu_t \mathbf{a} + \nu_t \mathbf{a}^+ \quad (16)$$

Substituting (15) into (12) we obtain  $\mu_t$  and  $\nu_t$  as

$$\mu_t = \mu(t)\mu_0 + \nu(t)\nu_0^* \quad (17)$$

And

$$\nu_t = \mu(t)\nu_0 + \nu(t)\mu_0^* \quad (18)$$

The evolved state is an eigen state of operator  $\mathbf{b}(t)$

$$\mathbf{b}(t)|\beta, \mu_t, \nu_t\rangle = \beta|\beta, \mu_t, \nu_t\rangle \quad (19)$$

(12-19) is used in calculating measurable quantities. The relaxation behaviour of the field is obtained by calculating the time dependence of the expectation value of the photon number operator in the state of the field. The expectation value is given by

$$\langle \mathbf{a}^+ \mathbf{a} \rangle = \langle \beta, \mu_t, \nu_t | \mathbf{a}^+ \mathbf{a} | \beta, \mu_t, \nu_t \rangle \quad (20)$$

The right hand side of (20) is evaluated by first inverting (16) and then using commutation relations and (19). The result has non-oscillatory as well as oscillatory time dependence. The non-oscillatory part determines the relaxation or decay behaviour. It has terms of the forms  $(1 + \lambda_0 t)^{-1}$  and  $(1 + \lambda_0 t)^{-2}$ . The oscillatory part occurs with frequency  $\omega$  and is too fast to be observed. Integrating the expression over a time interval  $\frac{2\pi}{\omega}$  averages it out. The variation of  $(1 + \lambda_0 t)$  during integration over the interval  $\frac{2\pi}{\omega}$  can be ignored beyond  $t \gg \frac{1}{\omega}$ . This

condition is satisfied in biophoton emission where the frequency is in optical range ( $\omega \approx 10^{15} \text{ s}^{-1}$ ) and measurements are beyond  $t = 1 \text{ ms}$  [39]. The expectation value  $\langle \mathbf{a}^+ \mathbf{a} \rangle$  averaged over the fast mode gives the number of photons  $n(t)$  detected at time  $t$  as

$$n(t) = B_0 + \frac{B_1}{1 + \lambda_0 t} + \frac{B_2}{(1 + \lambda_0 t)^2} \quad (21)$$

The coefficients  $B_0$ ,  $B_1$  and  $B_2$  are explicit expressions of  $\lambda_0$  and parameters  $\beta, \mu_0$  and  $\nu_0$ . The parameters are situation specific and may depend upon many factors. The values of the coefficients may change from experiment to experiment. Since we are unable either to prepare or choose a system with its field in a non-squeezed state, it is difficult to extract meaningful information about the system from these coefficients. In contrast,  $\lambda_0$  is sensitive to the state of the field and is a stable quantity. It may provide significant information about the system. The data should be analyzed to estimate its value.  $\lambda_0$  can be determined from the measurements of  $n(t)$  provided it is less than  $10^6 \text{ s}^{-1}$ . This restriction arises because for  $\lambda_0 > 10^6 \text{ s}^{-1}$  and  $t > 1 \text{ ms}$ , one can replace  $(1 + \lambda_0 t)$  by  $\lambda_0 t$  and can absorb  $\lambda_0$  in the coefficients  $B_1$  and  $B_2$ . The error in the replacement is less than 0.1%. Besides, the system will relax very quickly for large values of  $\lambda_0$  and one will observe only a constant flux given by the contribution of  $B_0$ . If

$\lambda_0 \ll 10^6 \text{ s}^{-1}$ , then we can express the expression in eq.(20) in term of a dimensionless parameter  $\frac{\lambda_0}{\omega}$  less than  $10^{-9}$ . The expansion of (21) in this parameter has terms up to fourth order only, i.e.

$$n(t) = \sum_{m=0}^4 C_m \left( \frac{\lambda_0}{\omega} \right)^m \quad (22)$$

In the above equation only the term  $C_0$  is significant due to small value of expansion parameter. It is given by

$$C_0 = |\nu_0|^2 + |\beta|^2 (1 + 2|\nu_0|^2) \quad (23)$$

It is independent of t and produces a constant flux of photons.  $C_0$  gives a dominant contribution to n (t) provided  $|\nu_0| \gg \frac{\lambda_0}{\omega}$  or  $|\beta| \gg \frac{\lambda_0}{\omega}$ .

However, if both  $|\nu_0|$  and  $\beta$  become of the order of  $\frac{\lambda_0}{\omega}$ , then the expansion terms in (22) need to be rearranged. The rearranged expansion is given by

$$n(t) = |\nu_0|^2 + |\beta|^2 + \frac{\lambda_0}{\omega} \text{Im}(\mu_0 \nu_0) + \frac{\lambda_0^2}{4\omega^2} \left( 1 + \frac{1}{(1 + \lambda_0 t)^2} \right) + O\left( \frac{\lambda_0}{\omega} \right)^3 \quad (24)$$

Eq. (24) gives leading order contributions to the three coefficients of (21).  $B_0$  and  $B_2$  are non-vanishing but  $B_1$  vanishes in the expansion up

to the order  $\left( \frac{\lambda_0}{\omega} \right)^2$ .

We point out that eq. (24) is the only observable decay behaviour of the bi-photon field in this model. It has a  $(1 + \lambda_0 t)^{-2}$  term along with a constant rate of photon emission. The strength of decaying and constant terms depends upon the choice of parameters. For example if  $\mu_0 \cong 1$ ,  $\nu_0 = \frac{-i\lambda_0}{2\omega}$  and  $\beta = 0$ , then the constant component of the flux becomes zero. Similarly for the choice  $\mu_0 = 1, \nu_0 = 0$  and  $\beta$  arbitrary, the contribution of constant terms is never less than the contribution of the decaying terms. In this choice the state of the field at  $t = 0$  is a coherent state of the photon. Equations (23) and (24) can be combined in a single formula for phenomenological analysis. It gives  $n(t)$  as

$$n(t) = B_0 + \frac{B_2}{(1 + \lambda_0 t)^2} \quad (25)$$

Gu<sup>[22]</sup> has also obtained similar expression in an exciplex model after several approximations. Our approach is much simpler and tractable.

The uncertainty product is calculated using (7). We give the result for the field initially in a coherent state evolving into a squeezed state. It has  $\nu_0 = 0$  and gives

$$\Delta x \Delta p_x = \frac{\hbar}{2} \sqrt{1 + \Omega(t)^2} \quad (26)$$

, where

$$\begin{aligned} \Omega(t) = & \frac{\lambda_0}{\omega} \left\{ 1 + \frac{\lambda_0^2}{2\omega^2(1+\lambda_0 t)^2} \right\} \\ & - \frac{\lambda_0}{\omega} \cos 2\omega t \left\{ \frac{1}{(1+\lambda_0 t)} + \frac{\lambda_0^2}{2\omega^2(1+\lambda_0 t)^2} \right\} \\ & - \frac{\lambda_0^2}{2\omega^2} \sin 2\omega t \left\{ \frac{2}{(1+\lambda_0 t)} + \frac{1}{(1+\lambda_0 t)^2} \right\} \end{aligned} \quad (27)$$

The oscillatory behaviour has not been integrated out in the above expression. The contribution of  $\Omega(t)$  is very small for  $\frac{\lambda_0}{\omega} \ll 1$ . The uncertainty product of the packet does not grow with time and it remains nearly a minimum uncertainty packet. It does not suffer appreciable attenuation due to quantum evolution. It can therefore be used for efficient signal transmission and communication <sup>[43,39]</sup>. The behavior of the uncertainty product for the field initially in a squeezed state ( $\nu_0 \neq 0$ ) is given by a more complicated expression but is similar to the case  $\nu_0 = 0$ . We have also determined the nature of photon statistics by calculating  $Q$  with the help of (8).  $Q$  is non-zero but small. It indicates that the distribution is not strictly Poissonian. However, the deviations are observed to be small.

## Chapter 5

### Biophoton signal from *Tagetes Patula*

**1.1 Implications of the model:** The mathematical model developed in the last chapter can be applied to explain the behaviour of the biophoton signals emitted different living systems. The model predicts the relaxation behaviour of the form

$$n(t) = B_0 + \frac{B_2}{(1 + \lambda_0 t)^2} + \frac{B_1}{(1 + \lambda_0 t)} \quad (1)$$

Eq. (1) is our main result. It explains the spontaneous as well as stimulated biophoton emissions in a unified framework in all living systems. Quite often only one time dependent is significant term (either  $B_2 \gg B_1$  or  $B_2 \gg B_1$ ). In the case of the biophoton signals from the flowers of *Tagetes patula* (marigold) observed by us, we have found the contribution of  $B_1$  to be negligible. We have, therefore, discussed below this situation in detail. There remain only three unknown parameters in eq.(1). One parameter ( $B_0$  or  $B_2$ ) is fixed by the normalization of the data. This leaves only two parameters  $\lambda_0$  and ( $B_0$  or  $B_2$ ) to fit the experimental data. The model predicts a constant flux of biophotons in time for  $t \ll \frac{1}{\lambda_0}$  or  $B_0 \gg B_2$ . This is an important feature of our model. It has not been predicted so far. All biological systems exhibit this feature of constant flux in biophoton emission. Energy emitted in biophoton emission is supplied by the metabolic activities of the system. The mechanism of energy transfer from the living system to its field is unknown. We have modelled only part of the Hamiltonian that gives

the evolution of the electromagnetic field. This part has explicit time dependence and it alone cannot conserve energy. Energy conservation is ensured by the living system as a whole, which is responsible for the existence of the field in a squeezed state.

The model contains the relaxation behaviour of the form  $(1 + \lambda_0 t)^{-2}$  for  $B_2 \gg B_0$ . This is the only form of relaxation behaviour occurring in our model. Such behaviour was observed in numerous systems <sup>[22,25,44,45]</sup>. These observations led to the idea of frequency stable damped oscillator initially in a classical state <sup>[42]</sup>. We have borrowed the form of damping and formulated a quantum mechanical framework for understanding biophoton emission. The framework correctly gives the observed decay behaviour. It may be noted that non-exponential decay rules out the origin of biophoton from uncorrelated excited states of subsystems or from chemical reactions.

The parameters  $B_0$  and  $B_2$  depend upon the quantum state of the field and are holistic in character. They need not be extensive variables. They depend upon physiological and environmental factors. The dependence has not been quantified so far. Changes in biophoton signal with physiological and environmental conditions have been observed <sup>[45]</sup>. Our model attributes these changes to the values of  $B_0$  and  $B_2$ . The detailed shape of the biophoton signal is therefore situation specific. This is a unique feature of our model and it offers a possibility to use the biophoton signal as a tool in extracting information about physiological and environmental factors affecting the system. Using the biophoton signal, it may be

possible to discriminate among biological samples (carrot, milk, egg, etc) produced or reared under different conditions from the same species or stock, where chemical or biochemical techniques fail to differentiate <sup>[46]</sup>.

Light induced biophoton signals from living systems show characteristic non-exponential decay behaviour. The decay has a long tail in which the photons are emitted with almost constant flux. Radiation emitted in both regions is called by the common name biophotons. They are observed to be more intense in photosynthetic systems.

**5.2 Biophoton Signal of *Tagetes Patula*:** A non-photo synthetic system called flowers of *tagetes patula* is selected for study. Nine flowers varying in colour and size were plucked randomly from different plants. The light induced photon emission was measured continuously for 200s in the Photon Image Acquisition System (PIAS, HAMAMATSU). The details of the experimental set up and the actual procedure have been described elsewhere <sup>[27]</sup>. The signal became very weak after 200s and approaches the regime of constant flux. The measurements were repeated after every hour for 6 hours and subsequently once a day for next seven days. We measured the relaxation behaviour of each flower 14 times, spread over 8 days and obtained 126 different sets of data. The data of each set was analysed assuming a single exponential decay, double exponential decay and our model. The parameters in different models were determined by minimizing the  $\chi^2$ , function. A single exponential decay gave a large value of  $\chi^2$  and could not

produce the shape of the signal. The decay with two exponentials are parameterized by

$$n(t) = E_1 \exp(-\lambda_1 t) + E_2 \exp(-\lambda_2 t) \quad (2)$$

Where  $E_1$ ,  $E_2$ ,  $\lambda_1$  and  $\lambda_2$  are constants. Both Eqs. (1) And (2) was able to reproduce the shape of the signal and gave similar values for Chi-square. Chi-square per degree of freedom was around 1.2 in various sets of data. The values of  $B_0$  were small and negligible. The values of the coefficients  $E_1$ ,  $E_2$  and  $B_2$  were different for different flowers. Even for the same flowers the values of these coefficients decreased with time. The decrease indicated the degradation of a flower after plucking. The values decreased by two orders of magnitude in eight days. Perhaps they can be used to estimate the amount of degradation of the system. One expects the  $\lambda$  to be constant. The data from 126 decays gave  $\lambda_0 = (0.040 \pm 0.011)\text{S}^{-1}$ ,  $\lambda_1 = (0.080 \pm 0.041)\text{S}^{-1}$  and  $\lambda_2 = (0.015 \pm 0.003)\text{S}^{-1}$ . The term corresponding to  $\lambda_1$  is dominant in the two exponential decay model. But we obtained a significantly larger standard deviation in its determination. The values of  $\lambda_0$  and  $\lambda_2$  were distributed normally, but the values of  $\lambda_1$  were not. It suggests that Eq. (2) may simply be a parametric fit while Eq. (1) has deeper significance.

The quality of our fit is indicated in three representative cases in Fig.21. The number of photons detected in each second is plotted as a function of time elapsed after 10s exposure of the flower to white light. Photon counts measured every 3 seconds. Continuous lines join observed points. Predictions of the model are

depicted by dotted curves. The flower was plucked from a plant and kept in a sample holder inside the laboratory. The three cases correspond to measurements with the same flower on the first, fourth and eighth day of plucking. The data are well reproduced in these cases in our model. It is also true for all other sets of data. Agreement of the data in our model is particularly good for fresh flowers emanating a strong signal. Deviations are pronounced in weaker signals where the signal to noise ratio is less than 2. Our model correctly reproduces the shape of the signal even after the decrease in its strength by two orders of magnitude due to natural degradation.

The model proposes a new framework to represent and explain biophoton emission data. We feel that the earlier data showing non-exponential decay should be re-examined in this framework and future experiments should be planned to determine the dependence of the coefficients of the model on physiological and environmental factors.

Non-classical nature of biophotonic light is an important assumption of the model. It can be established by determining photo count statistics and by performing photon correlation experiments. Photo count statistics was determined in the region of constant flux in a few systems. The distribution was non-thermal and mostly Poissonian <sup>[25]</sup>. The probability of zero photon emission for a time interval ranging from 10 $\mu$ s to 10ms in light induced biophoton emission from photosynthetic systems <sup>[47]</sup> has now been measured. The measuring conditions were arranged in such a way that the difference in the predictions of thermal and Poissonian distributions was maximized. The data agree with the prediction of

Poissonian distribution. The results of both measurements require a non-classical nature of biophoton field. There are now three different types of measurements performed on different systems using different detectors indicating the existence of non-classical light. Perhaps, the biophoton field is indeed in a squeezed state of light.

There are many types of squeezed states possible for an electromagnetic field. We have taken into consideration only the two-photon coherent states. The motion of damped harmonic oscillator with time dependent mass and damping terms gives the evolution of our state. We did not consider the excited states (number states) of quasi particles and the states obtained by squeezing and displacing number states of photon. The algebraic complexity forced us to abandon this venture.

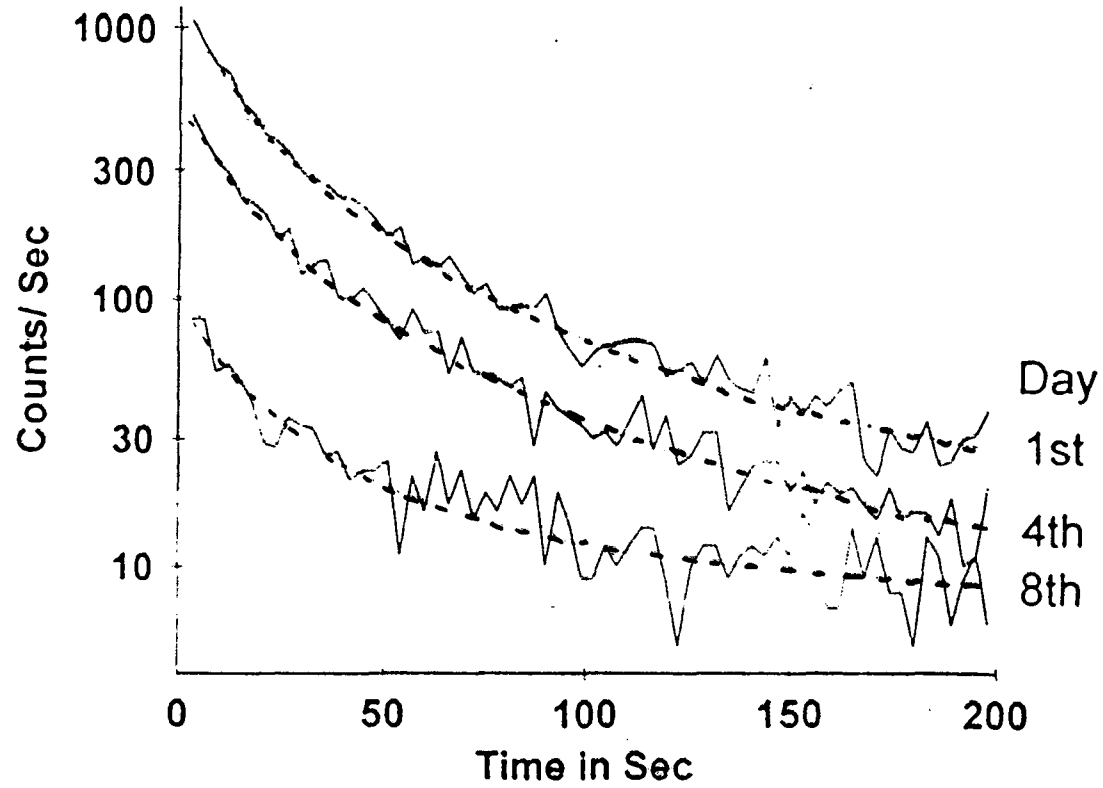


Fig: 21. Relaxation behaviour in the light induced emission from flowers of Tagetes Patula

## References

1. D. Swinbanks: Body light points to health, *Nature* **324**(1986) p.203.
2. B.Jezowska-Trzebiatowska, B.Kochel, J.Slawinski and W.Strek (eds.): *Photon Emission from Biological Systems* (World Scientific, Singapore, 1986).
3. F.A.Popp, A.A. Gurvich, H.Inaba, G.Cilento, R.van Wijk, W.B.Chwirot and W.Nagl, Biophoton Emission (Multi-author Review). *Experientia* **44** (1988) p. 543-600.
4. A.G.Gurvich, and L.D.Gurvich, Die mitogenetische Strahlung (Fischer Verla, Jena 1959).
5. A. Kohn: *False Prophets: Fraud and Error in Science and Medicines*, Blackwell, Oxford,(1986).
6. A. Kohn: *False Prophets: Fraud and Error in Science and Medicines*, Blackwell, Oxford,(1986).
7. M. Schubert and B. Wilhelmi: Non-linear Optics And Quantum Electronics, John Wiley & Sons, Inc., U.S.A, April (1986) p. 4.
8. D.F.Walls and G.J.Milburn, Quantum Optics, Springer-Verlag, Berlin, (1994) p. 8.
9. R.Loudon, Quantum Theory of Light, Oxford University Press, New York, 1983, pp. 129-133.

10. S.J. Van Eck, J.I. Cirac, p. Zoller, Phys. Rev. Lett. **78**, 4293 (1997).
11. P. Domokos, M. Brune, J.M. Raimond and H.Haroche, Euro. Phys. J. DI, 1998, 1-4.
12. R.J. Glauber, Phys. Rev. **B 1**, 2766, (1963).
13. R.J. Glauber, E.C.G. Sudarshan, Fundamentals of Quantum Optics, W.A. Benjamin, Inc. New York, 106, (1968).
14. C.M. Caves, Phys. Rev. D **23**, 1693 (1981).
15. A.F. Pace, M.J. Collett, D.F. Walls, Phys. Rev. **A47** (1993) p.3173.
16. L.A. Wu, M. Xiao, H.J. Kimble, J. Opt. Soc. Am. **B4** (1987) p.1465.
17. R. Hanbury-Brown, R.W. Twiss: Nature, **177**, 27 (1956).
18. C. H. Bennett et al. Teleportation protocol, Phys. Rev. Lett. **70**, 1895 (1993).
19. H.P. Yuen, Phy. Rev. **A13**, 2226 (1976).
20. B. Ruth, in: F.A. Popp, U.warnke, H.L. Koenig, W. Peschka (Eds.), Electromagnetic Bioinformation, Urban and Schwarzenberg, Munich, 1989, pp. 128-143.
21. F.A. Popp, in: F.A. Popp, U.Warnke, H.L. Koenig, W. Peschka (Eds.), Electromagnetic Information, Urban and Schwarzenberg, Munich, 1989, pp.144-167.

22. Q. Gu, in: F.A. Popp, K.H. Li, Q.Gu (Eds.), *Recent Advances in Biophoton Research and its Applications*, World Scientific, Singapore, 1992, pp. 59-112.
23. J. Slawinski, *Experientia*, **44**, (1988), 559.
24. P.A. Jursinic, in: J.A. Govindji, D.A. Frog (Eds.), *Light Emission by Plants and Bacteria*, Academic Press, New York, 1986, pp. 291.
25. F.A. Popp, in: F.A. Popp, K.H. Li, Q. Gu (Eds.), *Recent Advances in Biophoton Research and its Applications*, World Scientific, Singapore, 1992, pp.1-46.
26. W.B. Chwirot, *Experientia*, **44**, 1988, pp.594.
27. R.P. Bajpai, P.K. Bajpai, *J. Biolum. Chemilum.* **7**, 1992, pp.117.
28. J. Lavorel, in: R.Govindji (Ed.), *Bioenergetics of Photosynthesis*, Academic Press, New York, 1975, pp. 225.
29. B.G. Mathew, S. Kumar, *Experientia*, **48**, 1992, pp.309.
30. Q. Gu, F.A. Popp, *Experientia*, **48**, 1992, pp.1069.
31. F.A. Popp, W. Nagl, K.H. Li, W. scholz, O. Weingaertner and R. Wolf, *Biophoton Emission: New Evidence for Coherence and DNA as Source. Cell Biophys.* **6** (1984) pp. 33-52.
32. F.A. Popp, in: F.A. Popp, K.H. Li, Q. Gu (Eds.), *Recent Advances in Biophoton Research and its Applications*, World Scientific, Singapore, 1992, pp. 47-58.

33. K.H. Li, F.A. Popp, Phys. Lett. A **93** (1983) pp. 626.
34. F.A. Popp, B. Ruth, W. Bahr, J. Boehm, p. Grass, G. Grolig, M. Ratemeyer, H.G. Schmidt and P.Wulle, Collective phenomena, **3**, (1981) pp.187.
35. F.A. Popp, in Disequilibrium and Self-Organisation, ed. C.W. Kilmister (D. Reidal Publishing Company, Dordrecht, 1986.
36. A. Jannussis and V. Bartzis, IL Nuovo Cimento **B 102** (1988) pp. 33.
37. F.A. Popp, in: F.A. Popp, K.H. Li, Q. Gu (Eds.), Recent Advances in Biophoton Research and its Applications, World Scientific, Singapore, 1992, pp.113-155.
38. D.F. Walls, Nature, **306**, (1983) pp.141.
39. R.J. Glauber, Phys. Rev. **131** (1963) pp.2766.
40. L.Mandel, Optical Communication, **42** (1982) pp. 437.
41. I.A. Pedrosa, Phys. Rev. **D36** (1987) pp.1279.
42. F.A. Popp, K.H. Li, Internat. J. Theoret. Phys. **32** (1993) pp.1573.
43. H.P. Yuen, J. shapiro, IEEE Trans. Inform. Theo. **IT26** (1980) pp.78.
44. F. Musumeci, M. Godlewski, F.A. Popp, M.W. Ho, in: F.A.Popp, K.H. Li, Q.Gu (Eds.), Recent Advances in Biophoton Research and its Applications, World Scientific, Singapore, 1992, pp. 327-344.
45. F.A. Popp, Q. Gu, K.H. Li, Mod. Phys. Lett. **B8** (1994) 1269.

46. K. Lambing, in: F.A. Popp, K.H. Li, Q. Gu (Eds.), *Recent Advances in Biophoton Research and its Applications*, World Scientific, Singapore, 1992, pp. 393-413.
47. R.P. Bajpai: *J. Theor. Biol* (1999) Coherent nature of photon in delayed luminescence of leaves, Submitted **198**, 287-299.